Ma *et al. Energy Mater* 2022;2:200027
DOI: 10.20517/energymater.2022.23

Energy Materials

Review

Open Access

Check for updates

Insights into the electrochemical performance of metal fluoride cathodes for lithium batteries

Delong Ma[1], Ruili Zhang[1], Xun Hu[1,*], Yang Chen[1], Chenfa Xiao[1], Fei He[1], Shu Zhang[2], Jianbing Chen[3], Guangzhi Hu[4,*]

[1]School of Material Science and Engineering, University of Jinan, Jinan 250022, Shandong, China.
[2]Joint International Research Laboratory of Biomass Energy and Materials, College of Materials Science and Engineering, Nanjing Forestry University, Nanjing 210037, Jiangsu, China.
[3]Research Academy of Non-metallic Mining Industry Development, Materials and Environmental Engineering College, Chizhou University, Chizhou 247000, Anhui, China.
[4]School of Materials and Energy, Institute for Ecological Research and Pollution Control of Plateau Lakes, School of Ecology and Environmental Science, Yunnan University, Kunming 650091, Yunnan, China.

Correspondence to: Prof. Xun Hu, School of Material Science and Engineering, University of Jinan, No. 336 West Nanxinzhuang Road, Jinan 250022, Shandong, China. E-mial: Xun.Hu@outlook.com; Prof. Guangzhi Hu, School of Materials and Energy, Institute for Ecological Research and Pollution Control of Plateau Lakes, School of Ecology and Environmental Science, Yunnan University, No. 2 North Cuihu Road, Wuhua District, Kunming 650091, Yunnan, China. E-mail: guangzhihu@ynu.edu.cn

How to cite this article: Ma D, Zhang R, Hu X, Chen Y, Xiao C, He F, Zhang S, Chen J, Hu G. Insights into the electrochemical performance of metal fluoride cathodes for lithium batteries. *Energy Mater* 2022;2:200027. https://dx.doi.org/10.20517/energymater.2022.23

Received: 1 May 2022 **First Decision:** 27 May 2022 **Revised:** 24 Jun 2022 **Accepted:** 15 Jul 2022 **Published:** 28 Jul 2022

Academic Editors: Yuping Wu, Keyu Xie **Copy Editor:** Tiantian Shi **Production Editor:** Tiantian Shi

Abstract

In recent years, energy storage and conversion have become key areas of research to address social and environmental issues, as well as practical applications, such as increasing the storage capacity of portable electronic storage devices. However, current commercial lithium-ion batteries suffer from low specific energy and high cost and toxicity. Conversion-type cathode materials are promising candidates for next-generation Li metal and Li-ion batteries (LIBs). Metal fluoride materials have shown tremendous chemical tailorability and exhibit excellent energy density in LIBs. Batteries based on such electrodes can compete with other envisaged alternatives, such as Li-air and Li-S systems. However, conversion reactions are typically multiphase redox reactions with mass transport phenomena and nucleation and growth processes of new phases along with interfacial reactions. Therefore, these reactions involve nonequilibrium reaction pathways and significant overpotentials during the charge-discharge process. In this review, we summarize the key challenges facing metal fluoride cathode materials and general strategies to overcome them in cells. Different synthesis methods of metal fluorides are also presented and discussed in the context of their application as cathode materials in Li and LIBs. Finally, the current challenges

and future opportunities of metal fluorides as electrode materials are emphasized. With continuous rapid improvements in the electrochemical performance of metal fluorides, it is believed that these materials will be used extensively for energy storage in Li batteries in the future.

Keywords: Metal fluorides, cathodes, Li-ion batteries, conversion reaction

INTRODUCTION

The story of Li batteries started in the 1950s when lithium metal was used as an anode material in non-aqueous primary cells[1-5]. The high energy densities and low chemical potential of Li/Li^+ (-3.04 V *vs*. SHE) make Li batteries the most favorable devices for energy storage. Later, in 1977-1979, coin cells based on a TiS_2 cathode, Li-alloy anode, and organic electrolyte ($LiClO_4$-dioxolane) were successfully commercialized by Exxon[5], followed by comprehensive research on a series of Li-free cathode materials, including TaS_2, MoS_2, TiS_2, VS_2, NbS_2 and CrS_2[5,6]. Unfortunately, secondary batteries with Li metal anode carry a risk of explosion due to the growth of lithium dendrites that can pierce the separator during cycling. To solve this problem, the Li-metal anode was replaced by a carbon anode to assemble powerful and safe Li-ion batteries (LIBs). Presently, the fast-growing market requires next-generation rechargeable Li and LIBs to charge faster, have higher energy density and be cheaper and safer. Battery materials with high capacity are therefore being largely developed and explored in advanced LIBs. Unfortunately, many of the cathode materials, like lithium cobalt oxide, lithium nickel oxide, and $LiMn_2O_4$, used nowadays for traditional LIBs have limits in electrochemistry, such as low energy density, safety hazards, high price, and environmental issues. Recently, owing to the progress in solid electrolyte research, Li-metal batteries are expected to make a comeback[3,7-9] as the anode material is based on metal Li, and it is therefore not essential for the cathode to contain Li.

Efforts to prepare Li-free cathodes have increased in recent years because of the perspective advantages of Li-free cathode materials, such as eco-friendliness, low cost, and high capacity. As one type of Li-free cathode material, conversion-type metal fluoride cathodes, which exhibit low cost and high theoretical capacity, have recently attracted substantial attention[10]. Mainly, Li-S battery systems have been widely considered, but S cathodes still face several issues, such as the dissolution of intermediate lithium polysulfides in the electrolyte and low volumetric energy density[11,12]. The high ionicity of the M-F bond favors a higher reaction voltage compared to their oxide and sulfide counterparts[13]. Therefore, metal fluoride-based cathodes (e.g., NiF_2, FeF_2, FeF_3 and so on) hold significant promise for energy storage applications[14-17].

Figure 1A shows the theoretical specific capacities and operational voltages for Li-free cathodes[3]. It is found that metal fluorides have the highest electromotive force due to the high electronegativity of F. Metal fluoride cathodes also show high gravimetric (> 1600 Wh kg^{-1}) and volumetric (> 6700 Wh L^{-1}) energy densities [Figure 1B and C] compared to LIBs cathodes, such as $LiNi_{0.5}Mn_{1.5}O_4$ and sulfur. Figure 1D shows the cell energy densities of transition metal fluorides, with values of 1172 Wh kg^{-1} (2178 Wh L^{-1}) for CuF_2 and 1125 Wh kg^{-1} (1782 Wh L^{-1}) for FeF_3. It is noteworthy that the real energy densities will decrease because a higher percentage of carbon and solid-state electrolytes need to be mixed with the cathodes and anodes to improve the ionic and electron conductivity and achieve better battery performance. Nevertheless, it still remains much higher than that of current LIBs (150-300 Wh kg^{-1}).

Recently, Na- and K-ion batteries are becoming more promising for large scale energy-storage, which can alleviate the concerns regarding the scarcity of Li resources. Although the well-established LIB technology

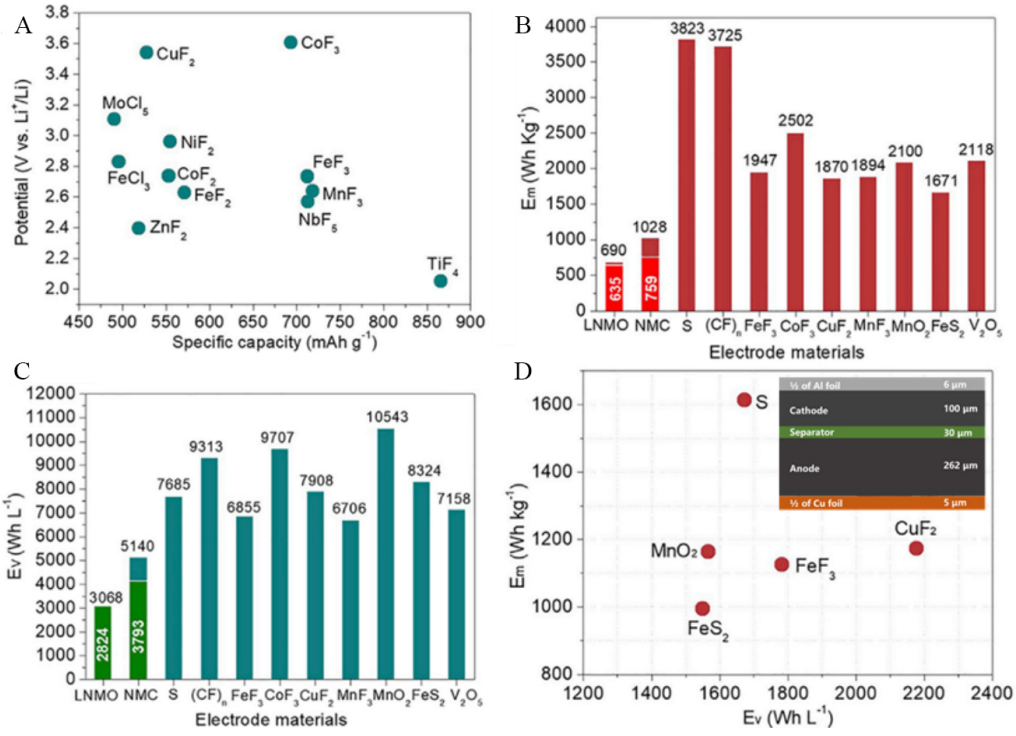

Figure 1. (A) Theoretical specific capacity and operational voltage for conversion cathodes. (B) and (C) Gravimetric and volumetric energy densities of Li-free cathodes ($LiNi_{0.5}Mn_{1.5}O_4$ denoted as LNMO and $Li(NiMnCo)_{1/3}O_2$ denoted as NMC). (D) Energy density of solid-state Li batteries with different cathodes: FeF_3; CuF_2; MnO_2; S (inset shows a schematic of a solid-state battery). Reproduced from Ref.[3] with permission. Copyright 2019 Elsevier Inc.

can be exploited for them, their energy density is generally lower than that of LIBs. Therefore, developing high-performance electrode materials is also one of the research emphases for Na- and K-ion batteries. Metal fluorides (FeF_2, FeF_3 and CuF_2) exhibit promising electrochemical performance, which could be the solution for batteries in the future.

In this review, we summarize the key challenges facing metal fluoride cathode materials and general strategies to overcome them in cells. Different synthesis methods for these materials are described and their electrochemical applications as cathode materials in Li batteries and LIBs are discussed. Finally, the current challenges and future opportunities of metal fluorides as electrode materials are emphasized. We provide a conclusive review of the recent progress made for the rational design of metal fluoride cathode materials in electrochemistry for energy storage in Li batteries.

CONVERSION REACTION MECHANISM IN METAL FLUORIDE CATHODES

As one of the reaction pathways for batteries, conversion reactions involve the reduction of the active material into metallic nanoparticles and the formation of a Li compound, which is different from intercalation and alloying reactions. The generalized reaction formula can be expressed as:

$$M_aX_b + (b \cdot n)Li = aM + bLi_nX \text{ (M = metal; X = O, S, F or P)} \quad (1)$$

It should be noticed that an alloying reaction can take place when M is electrochemically active with Li (e.g., Sn, Sb or Zn), but this is beyond the scope of this review. Conversion-type electrode materials can usually achieve high reversible capacity because the specific capacity can be increased by using metal compounds

with high oxidation states. In addition, the working potential of these materials can be easily controlled by tuning the ionicity of the M-X bond.

In 1997, FeF_3 was first introduced as a prospective insertion-type LIB cathode material with a high theoretical energy density (237 mAh g^{-1}) based on a one-electron transfer and high discharge platform (average of 3 V). This opens up potential opportunities for next-generation LIBs[18]. Three decades later, the physical proof and stability of the metal fluoride conversion electrode have been separately demonstrated[19,20]. The past decade has witnessed tremendous advances in the preparation of metal fluoride electrode materials with improving electrochemical performance. The electrochemical performance, morphology, and particle size of some of the recent metal fluoride cathode nanomaterials are summarized in Table 1.

Among all the metal fluoride phases, FeF_3 cathodes with the multielectron transfer mechanism have received the most attention because of their high energy density and low cost. This material converts to nanocomposites of metal nanoparticles dispersed in a LiF matrix during the conversion reaction. Metallic iron may be nucleated to form nanosized Fe particles at the same initial atomic sites in the old phase, while newly formed LiF occupies the space around the metallic iron nanoparticles on the other side during lithiation. The diffusion coefficients of the anions and cations, the ionic and electronic conductivities of the new phase and the interfacial energies can be used to control the morphology of these cathode materials. Numerous studies have correlated the phase behavior in the insertion regime with reaction kinetics but with different mechanisms. The majority of studies indicate that the ReO_3 structure comprising corner-sharing FeF_6 groups transforms into the trirutile Li_xFeF_3 phase with an edge-sharing structure. There is a transformation that involves a considerable change in the Fe ordering and anion packing, albeit with different x values. Recently, Hua *et al.* revealed that FeF_3 lithiation is mainly a diffusion-controlled substitution mechanism. Furthermore, there is a clear topological relationship between the metal fluoride and F^- sublattices to that of LiF[7], as shown in Figure 2. FeF_2 is formed on the particle surface during the initial lithiation of FeF_3. The A-$LixFeyF_3$ phase (cation ordered and stacking disordered) is then formed along with FeF_2. This structure is related with α-/β-$LiMn^{2+}Fe^{3+}F_6$ and can topotactically transform to B- and then C-$Li_xFe_yF_3$ before forming LiF and Fe.

Iron fluoride (FeF_2) has also been widely studied as a model system for mechanistic studies. However, the lithiation of FeF_2 involves the formation of nanosized reaction products (LiF and Fe) and many possible intermediate phases. Karki *et al.* studied the conversion reactions in a single crystal of FeF_2. They reported a lithiation-driven topotactic transformation between the parent and converted phases by *in situ* visualization of the spatial and crystallographic correlation[9]. Specifically, conversion in FeF_2 cathode involves the transport of both Fe^{2+} and Li^+ ions within the F^- array and leads to the formation of nanosized Fe along specific crystallographic orientations of FeF_2, as shown in Figure 3. During the whole process, the retained F-anion framework creates a checkerboard-like structure, which can compensate the large volume change and thereby enable high cyclability in FeF_2.

Xiao *et al.* prepared single-crystalline, monodisperse FeF_2 nanorods through colloidal synthesis[8]. The nanorods presented near a theoretical capacity of 570 mA h g^{-1} and good cycling stability, solely through the use of an ionic liquid electrolyte (1 M LiFSI/Pyr1,3FSI). In this work, the conversion mechanism detailed reveals that the discharge and charge reactions are controlled by different mechanisms. As shown in Figure 4, the charge process is an interface-controlled reaction with the slow diffusion of Fe^{2+} through a rock-salt lattice. This is one of the main causes of inherently sluggish of voltage. In contrast, the discharge process is a diffusion-controlled reaction with the fast diffusion of Fe^0 through open channels. The study

Table 1. Electrochemical performance of metal fluoride cathode materials for LIBs

Electrode materials	Morphology	Particle size (nm)	Specific capacity (mAh g^{-1})	Cycle number	Ref./Year
FeF_3	layer hexagonal	-	80	-	[18] 1997
TiF_3	layer hexagonal	-	80	-	
VF_3	layer hexagonal	-	80	-	
MnF_3	layer hexagonal	-	80	-	
FeF_3	Film	200-300	571.2	30	[21] 2006
NiF_2	Nanoparticles	20-30	540	35	[22] 2008
$FeF_3{\cdot}0.33H_2O$	sponge-like	10	712	35	[23] 2010
Li_3FeF_6	prismatic particles	50	100	-	[24] 2010
$FeF_3{\cdot}0.33H_2O$	hierarchy	11	115	50	[25] 2011
CuF_2	Thin film	200	424	45	[26] 2011
FeF_2	Nanoparticles	< 5			[27] 2011
CuF_2		5-12			
FeF_2	Nanoparticles	9.1			[28] 2012
FeF_3	Nanoparticles		600		[29] 2012
FeF_3	Nanoparticles	5	~200	80	[30] 2012
FeF_3	Nanoparticles	55	140	50	[14] 2013
$FeF_3{\cdot}0.5H_2O$	Nanoparticles	10	115	100	[31] 2013
FeF_3	Nanospheres	70-100	222	50	[32] 2013
$FeF_3{\cdot}0.33H_2O$	Nanoparticles	10	140	100	[33] 2013
FeF_2	Films	850	511	10	[34] 2014
$FeF_{2.2}(OH)_{0.8}{\cdot}(H_2O)_{0.33}$	hexagonal-shaped particles	750	110	40	[35]2014
$FeF_3{\cdot}0.33H_2O$	Cylindrical	1000-2000	137	100	[36] 2014
$FeF_3{\cdot}0.33H_2O$	Nanopetal		123	50	[37] 2014
FeF_3	Particles		> 200	50	[38] 2014
$Fe_{1.9}F_{4.75}{\cdot}0.95H_2O$	Nanorods		148	100	[39] 2014
FeF_3	Nanocrystals	30		200	[40] 2014
CuF_2					[41] 2014
FeF_3	Powders		230	60	[42] 2015
LiF/FeF_3	Nanoparticles		260.1		[43] 2015
$FeF_3{\cdot}0.33H_2O$	Nanopetals	15	145	30	[44] 2015
MoF_3					[45] 2015
FeF_3	Powder		237	30	[46] 2015
B-$FeF_3{\cdot}3H_2O$	Nanoparticles		146.5	10	[47] 2015
FeF_3					[48] 2016
FeF_3	Nanoparticles		423		[49] 2016
MnF_2	Nanoparticles	50-200	489	100	[50] 2016
HTB-FeF_3			200-450	100	[51]2016
$FeF_3{\cdot}0.33H_2O$			250		[52] 2016
MnF_2	Nanorods		420	2000	[53] 2016
FeF_3	fusiform structure		137.3	100	[54] 2017
FeF_3	nanocrystals		93.8	500	[55] 2017
$FeF_3{\cdot}3H_2O$	Flower-like		172.3	50	[56] 2017
CuF_2					[57] 2017
FeF_3	Nanocrystal	5-20	155	100	[58] 2017
CoF_3	Nanopowder		390	14	[59] 2017
CuF_2	Nanostructures		270		[60] 2017
Li_2NiF_4	Nanospheres		548	40	[61] 2017
FeF_3	Nanosheets				[62] 2018
$FeF_3{\cdot}0.33H_2O$	Hierarchical				[63] 2018

FeF_3					[64] 2018
CoF_3			550		[65] 2018
FeOF	Cubic				[66] 2018
CuF_2	Nanoparticles	30-70			[67] 2018
LiF/Fe/Cu			375-400	200	[68] 2019
CuF_2					[69] 2019
$FeF_{2.2}(OH)$ 0.8					[70] 2019
FeF_2					[71] 2019
$FeF_3{\cdot}0.33H_2O$	Microspheres		172		[72] 2019
MnF_2	Nanolayer		296.8	100	[73] 2019
$FeF_3{\cdot}0.33\ H_2O$	Nanoparticles		190	50	[74] 2019
$FeF_3{\cdot}0.33H_2O$	Raspberry-like		284	100	[75] 2020

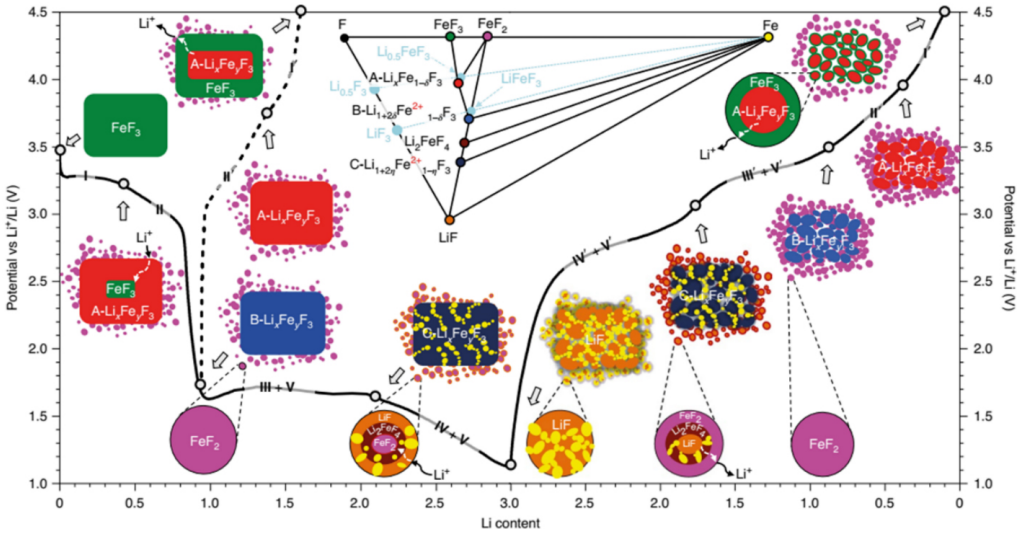

Figure 2. Reaction pathways of FeF_3-FeF_2 cathode. The reference phases in the phase diagram are indicated by light blue circles to show the positions of A- and B-Li_xFeyF_3, whose Fe concentration is off-stoichiometric. Reproduced from Ref.[7] with permission. Copyright 2021 Springer Nature.

suggests that voltage hysteresis is primarily a result of the reaction overpotential because the charge and discharge pathways are spatially and chemically symmetric. Based on the above results, we can mitigate the reaction hysteresis potentially through materials design. For example, a conductive bridge for electron transport can be made by doping or structural control to provide an enormous interface among nanosized products for the reversible conversion reaction. Regardless of the theoretical significant features of metal fluoride materials, many challenges still need to be resolved before these materials can achieve their desired performance characteristics. These challenges include low ionic and electron conductivities, voltage hysteresis, and unfavorable side reactions between active materials and electrolytes, all of which may lead to poor electrochemical performance and low Coulombic efficiency and energy efficiency.

LIMITATIONS OF CONVERSION MATERIALS AND STRATEGIES TO OVERCOME THEM

Low conductivity

Metal fluoride (FeF_3 and FeF_2)-based cathode materials are particularly promising materials due to their high volumetric and gravimetric capacities[17]. However, the strong ionic bond between M and F results in a large band gap, which makes metal fluoride materials poor electronic conductors[76,77]. The large interfacial

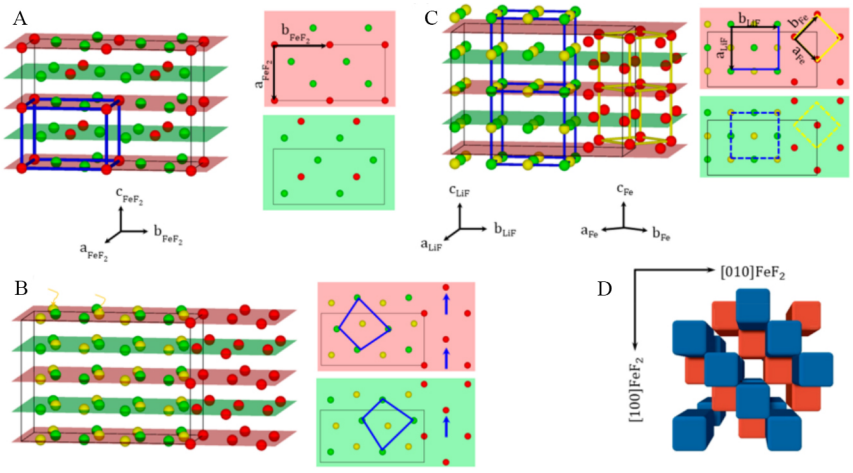

Figure 3. (A) Schematic illustration of structure of FeF_2 with Fe (red) and F (green). In the 3D view (left), the unit cell is outlined by thick blue lines. The thin black lines outline a 1 × 2 × 2 supercell. Alternative arrangement of Fe-F along the [001] direction in the unit cell is shown in the red and green planes. (B) Li (yellow) insertion along the [001] direction. (C) Expansion/contraction of Fe/LiF along different directions. (D) Perspective view of checkerboard arrangement of the converted Fe domains along the [001] FeF_2 direction. Reproduced from Ref.[9] with permission. Copyright 2018 American Chemical Society.

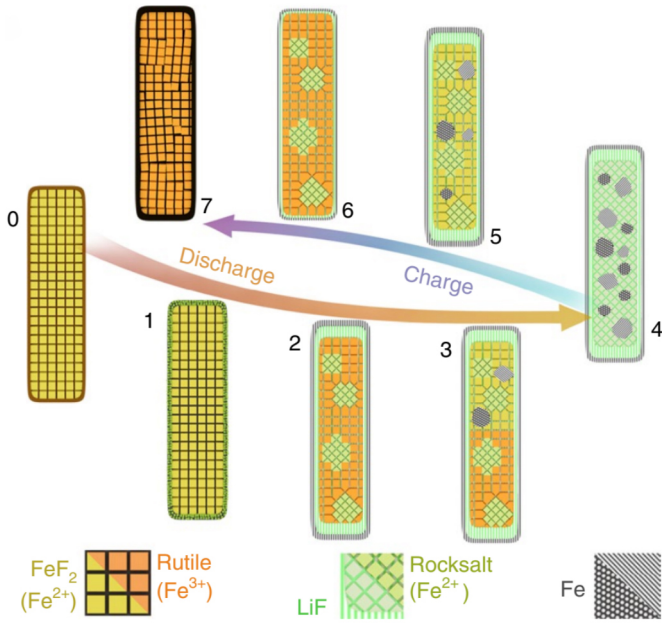

Figure 4. Schematic illustration of full discharge-charge mechanism for FeF_2 electrode. (1) Forming disordered Fe and LiF at the surface. (2) Forming trirutile and rocksalt phases throughout the interior accompanied by formation of Fe and LiF particles with double-layered shell. (3) The shell limits the propagation of the reaction to the [001], creating a boundary between the converted (iron containing) and unconverted regions. (4) Fully discharged state with Fe nanoparticles nucleated on the fluoride matrix. (5) Charging proceeds with the consumption of these Fe nanoparticles. (6) This is followed by the reconversion of the double-layered shell and the re-formation of a pseudo-single-crystalline rutile nanorod. Reproduced from Ref.[8] with permission. Copyright 2021 Springer Nature.

energy of Fe/LiF enhances the mass transport resistance, which hinders the development of large metals and LiF clusters during the cycling process. Furthermore, the harsh interactions between the electrolyte and metal fluoride cathode additionally improve the cell resistance and contribute to Fe degradation and dissolution, thus leading to rapid capacity fading upon cycling and irreversible structural changes along with low rate capability[19]. In addition, the slow separation of the Fe and LiF phases during the cycling

process may lead to capacity fading and cell polarization growth[27]. To overcome some of these problems, the development of various metal fluoride-based nanocomposites has been significantly explored[78,79]. Various conductive carbons, including graphene, carbon blacks, carbon fibers, carbon nanotubes (CNTs), and micro- and mesoporous carbons, have been greatly explored in such hybrid composite cathode syntheses and exhibited noticeable improvements in battery performance[17,80,81]. The poor electronic conduction of the electrode can be improved by the introduction of highly conductive materials, e.g., carbon and metal/metal oxides, which is effective in overcoming this limitation and positively improving the reversible capacity and stability of metal fluoride electrodes. The conductive species with an electron transport chain introduced into the active core material can maintain good electronic contact and effectively improve the kinetic behavior. Furthermore, the coating or adhesion of the external moieties on the active material surface efficiently hinders the side reaction and overpowers the dissolution.

Carbon-based metal fluoride nanocomposites

To improve the electrochemical performance and cycle stability, carbon-based nanocomposites have been used successfully because of their unique properties, such as high structural stability, high electronic conduction, large pore volume, and high surface area. Consequently, carbon composites with nanocomposites as core materials exhibit excellent electrochemical performance. Time, t, is proportional to the square of the diffusion length, L, during Li-ion diffusion, as shown in Equation (2)[82-84]:

$$t = L^2/D \qquad (2)$$

where D is the diffusion coefficient of Li ions.

The Badway group first reported carbon and metal fluoride nanocomposites (CMFNCs) as reversible cathodes to improve the electrochemical efficiency of metal fluorides[85]. They synthesized the CMFNCs via a ball-milling method, which showed a reversible specific capacity of ~600 mAh g^{-1} with a discharge voltage from 4.5 to 1.5 V. This result arises from the fact that the surface of nanosized crystals contains a number of surface defects that contribute significantly to improve the ionic and electronic activity. Nearly a third of the discharge capacity progressed in a cathode reduction reaction of Fe^{3+} to Fe^{2+} between 3.5 and 2.8 V, while the remaining specific capacity was provided by a two-phase conversion reaction at ~2 V, forming a finer Fe/LiF nanocomposite. Furthermore, the preliminary results of CoF_2, NiF_2, and FeF_2 CMFNCs were also used for comparison in the discussion of the electrochemical performance of the metal fluoride-based conversion reaction.

Despite intensive efforts, the poor cycling stability and partial reaction irreversibility have largely hampered the application of metal fluoride cathodes[18,19,86-88]. Therefore, an alternative method for the synthesis of cathode materials is desirable. For this reason, the intercalation of metal fluorides into a carbon matrix might be an effective approach to increasing the cycling performance. In particular, metal oxide-encapsulated carbon electrode materials have demonstrated superior cycling performances in LIBs[89]. Based on these concepts, the incorporation of metal fluoride into carbon materials, such as graphene, carbon fibers, CNTs, and mesoporous carbon materials, may lead to enhanced electrochemical properties. Therefore, Prakash *et al.* demonstrated ferrocene-based carbon-iron and LiF nanocomposite by pyrolysis of a mixture of LiF and ferrocene at 700 °C under an Ar atmosphere[90]. The composite was comprised of onion-type graphite structures and multi-walled CNTs, in which the LiF is dispersed within the carbon matrix and Fe_3C and Fe nanoparticles are incorporated in the carbon matrix [Figure 5A and B]. The nanocomposite presents a specific surface area of 82 m^2 g^{-1} and consists of both meso- (0.14 cm^3 g^{-1}) and micropores (0.025 cm^3 g^{-1}). The as-prepared cathode reached a reversible specific capacity of ~300 mAh g^{-1}

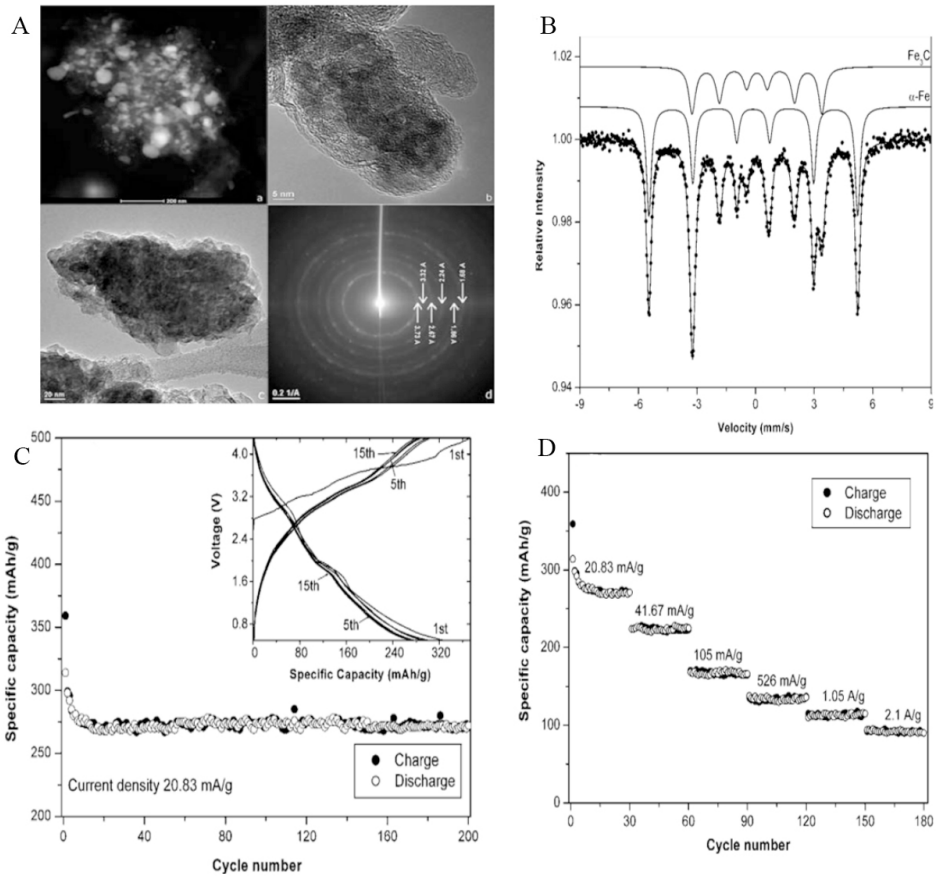

Figure 5. (A) TEM images of nanocomposite electrode after charging experiment. (B) Mossbauer spectrum of nanocomposite at 300 K. (C) Specific capacity and cycle performance of cathode. (D) Rate performance of as-prepared samples. Reproduced from Ref.[90] with permission. Copyright 2010 Royal Society of Chemistry.

at a current density of 20.83 mA g^{-1} with a potential range from 0.5 to 4.3 V. It showed good capacity retention (83.5% over 200 cycles) and excellent rate capability [Figure 5C and D]. Hence, due to its moderate capacity, more work is desired to optimize its reversible capacity, such as producing a uniform particle size/distribution, removing/reducing Fe_3C, reducing the carbon content, obtaining more Fe-encapsulated CNTs, and so on. Similarly, another group fabricated FeF_3 nanoflowers grown on CNT branch (FNCB)-based nanoarchitecture cathode materials by the functionalization of CNT surfaces[76]. The FNCBs exhibited improved electron transport and Li-ion storage when employed as cathode materials.

Graphene and reduced graphene oxide (RGO) stand out among carbon-based materials due to their outstanding mechanical properties and electrical conductivity[91-95]. Therefore, graphene sheets may be preferred conductive networks and building units to deliver facile electron pathways. A vapor-solid method was used for the first time to fabricate graphene-wrapped FeF_3 nanocrystals (FeF_3/G) as cathode materials [Figure 6A][96]. Compared to bare FeF_3, the as-prepared FeF_3/G nanocrystals supply an improved capacity of 155 mAh g^{-1} at a current density of 104 mA g^{-1}, as well as exhibiting superior rate capability and cyclic stability over 100 cycles, which could be attributed to the lower electrical resistance and buffering effect of the graphene layers [Figure 6B and C]. Liu *et al.* prepared an iron fluoride-reduced graphene nanocomposite cathode by a cost-effective low-temperature solution phase method[97]. Notably, the resulting iron fluoride-graphene nanocomposite cathode exhibited a high specific capacity of 210 mAh g^{-1} at 0.2C and demonstrated superior rate capability at high current densities (1, 2 and 5C).

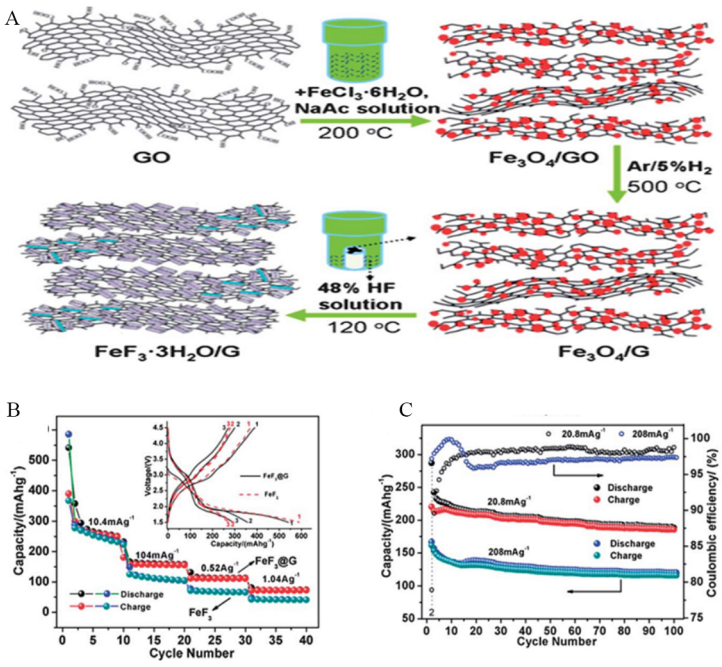

Figure 6. (A) Schematic illustration of fabrication procedure of FeF_3/G nanocomposite. (B) Rate capability and (inset) voltage profiles of FeF_3/G and bare FeF_3. (C) Cycling performance and Coulombic efficiency of FeF_3/G nanocomposite. Reproduced from Ref.[96] with permission. Copyright 2010 Royal Society of Chemistry.

Similarly, Qiu *et al.* reported the seeding of $FeF_3·0.33H_2O$ nanoparticles on RGO via an *in situ* approach and achieved enhanced cycling stability and high particle loading, attributed to the chemical tuning of the interfacial bonding between rGO and $FeF_3·0.33H_2O$ [Figure 7A and B][98]. Specifically, the $FeF_3·0.33H_2O$/rGO nanocomposites exhibit a higher discharge capacity of ~208.3 mAh g^{-1} at a current density of 0.5C and excellent cycle stability (133.1 mAh g^{-1} after 100 cycles at 100 mA g^{-1}) with 97% capacity retention [Figure 7C and D]. Later, highly uniform carbon-based nanocomposites with nanoconfined FeF_2 were successfully fabricated via a vacuum impregnation technique by the intercalation of a fluoride precursor with activated carbon powder[15]. Carbon pore walls prevent the physical separation of fluoride particles, accommodate fluoride volume changes during lithiation/delithiation, and supply holes or electrons to the electrochemical reaction sites during cell operation. When metal fluoride nanoparticles are confined into carbon nanopores, the nanocomposite displays dramatically superior electrochemical performance and cyclic stability in LIBs.

Previous research studies concentrated on introducing FeF_3 particles to the surface of carbon matrices or infusing them inside the nanopores of RGO, CNTs, and mesoporous carbon[30,97,99]. However, the synthesis of carbon matrices requires complex synthetic methods and is costly. Moreover, successfully creating the intimate contact between carbon matrices and FeF_3 nanoparticles is not easy, so avoiding the larger fraction of FeF_3 outside the inner pores is very challenging[100]. Nevertheless, a FeF_3-carbon composite with intimate contact between the conductive carbon matrices and FeF_3 nanoparticles has been fabricated by modified carbonization and polymerization processes. This method can effectively enhance the intimate contact between carbon and FeF_3 by the homogeneous mixing of $FeCl_3$ (FeF_3 precursors) with organic precursors (which can be converted into conductive carbon) at the molecular level. Thus, composites of FeF_3 nanoparticles wrapped in graphitized carbon were prepared via a facile polymerization process using citric acid ($C_6H_8O_7$), $FeCl_3$, and ethylene glycol as a carbon source, iron precursor, and crosslinking agent, respectively[101]. The as-synthesized graphitic carbon-coated FeF_3 composite displayed a capacity of

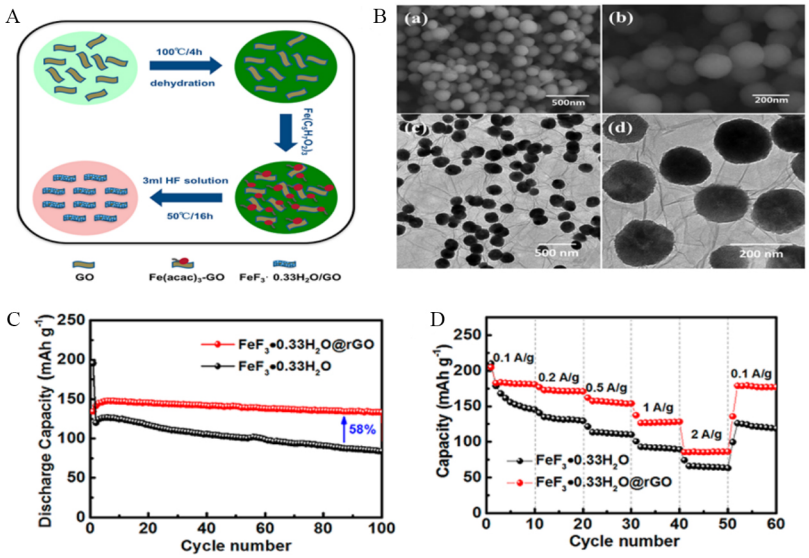

Figure 7. (A) Schematic illustration of preparation processes for FeF_3·0.33H_2O/rGO. (B) SEM and TEM images of FeF_3·0.33H_2O/rGO. (C) Cycling performance of FeF_3·0.33H_2O/rGO and FeF_3·0.33H_2O without rGO at a current density of 500 mA g^{-1}.(D) Rate performance of FeF_3·0.33H_2O/rGO and FeF_3·0.33H_2O NPs. Reproduced from Ref.[98] with permission. Copyright 2018 American Chemical Society.

188 mA h g^{-1} at initial discharge. After slow activation processes, the capacity finally reached 421 mAh g^{-1} in the voltage range from 1.5 to 4.5 V, which is superior compared to bare FeF_3. The enhanced cycling and rate performance of this nanocomposite were mainly accredited to the controlled size of the FeF_3 particles and the conductive graphitic carbon coated on the surface of FeF_3 during prolonged cycles.

In comparison to inorganic materials, various organic compounds have also been considered electrode materials but have received less attention due to the development of conductive polymers (CPs) and the achievement of intercalation compounds (e.g., $LiCoO_2$) in the 1980s as cathode materials for LIBs[102,103]. However, the intrinsic limits of intercalation compounds as cathodes for LIBs now desire innovation through the use of organic electrodes[104]. Therefore, carbonyl compounds are generally superior to CPs as electrode materials and are remarkable candidates for building low-cost, sustainable and functional energy storage systems[105]. For this reason, a hybrid FeF_3@$Li_2C_6O_6$/rGO nanocomposite was prepared by morphology control, intercalating RGO with spherical $Li_2C_6O_6$, followed by modification with a FeF_3 coating[106]. The as-prepared FeF_3@$Li_2C_6O_6$/rGO hybrid cathode displayed a superior cycling performance (320 mAh g^{-1} after 100 cycles), attributed to the coating of electrochemically active FeF_3 on the surface of $Li_2C_6O_6$, which successfully inhibited $Li_2C_6O_6$ dissolution in the electrolyte. This interface engineering approach and morphology control represent a feasible and scalable technique to effectively increase the rate performance and cycling properties of organic-based cathode materials. Recently, Reddy *et al.* synthesized carbon-FeF_2 nanocomposites by a facile one-step method at 250 °C, combining fluorinated carbon (CF_x) with iron pentacarbonyl -[$Fe(CO)_5$][107]. The resulting C-FeF_2 nanocomposites act as the cathode and achieve improved electrochemical properties. By reacting $Fe(CO)_5$ with four different CF_x precursors, they synthesized four different C-FeF_2 nanocomposites, which were made of carbon black, petcoke, carbon fibers, and graphite. The excellent electrochemical performance was also evaluated at 25 °C and 40 °C for high energy density LIBs.

Fu *et al*. reported an effective and versatile strategy for the development of metal fluoride-carbon nanofiber nanocomposites as flexible, free-standing cathodes[108]. The as-synthesized assembled FeF_3-C/Li cells exhibit a higher discharge capacity of 550 mAh g^{-1} at 100 mA g^{-1} and demonstrated excellent stability (> 400 cycles with no structural degradation). These promising characteristics can be effectively attributed to the robustness of the electrically conductive carbon network, the nanoconfinement of FeF_3 nanoparticles, reducing the irreversible separation and aggregation, the ultrafast pathways for electron transport and ion diffusion, and the inhibition of undesirable reactions between the liquid electrolyte and active materials.

Another effective and common method to enhance the electrochemical properties is the composite design of active materials. The first choice is always carbon-based metal fluoride composite electrodes. For instance, FeF_2 nanoparticles confined into carbon nanofibers can suppress the side reactions between FeF_2 and the electrolyte, thereby affording an enhanced electronic conductivity in the electrode and cycle stability over 400 cycles[108]. According to previously reported studies on battery electrode materials, the composite architecture design is a very capable approach to avoiding interactions between the active materials and electrolytes and accomplish fast transport in the electrode[109]. However, thus far, it is still a challenge to encapsulate nanosized FeF_2, FeF_3, CoF_2, and CuF_2 into a three-dimensional (3D) carbon matrix for the self-protection of electrodes and achieving fast electron and Li-ion transport. Simultaneously, the 3D architecture design can offer cathodes a high-active mass loading, high-rate performance, and good cycling stability. Therefore, Wu *et al*. prepared a FeF_3@C composite with a 3D honeycomb architecture by a simple and facile method[110]. The isolated FeF_3 particles with sizes of 10-50 nm were uniformly distributed in the 3D carbon honeycomb carbon framework, where the honeycomb carbon walls and hexagonal-like channels (cells) deliver sufficient conduction pathways for achieving fast ion diffusion and electron transport in FeF_3 cathodes. According to the results of the report, the as-prepared 3D honeycomb architecture FeF_3@C composite cathodes with high areal FeF_3 loadings (2.2 to 5.3 mg cm^{-2}) demonstrated an unprecedented rate capability of up to 100C and remarkable cycle stability within 1000 cycles, with high capacity retentions (95%-100%) within 200 cycles at 2C. As a result, it demonstrated that the 3D architecture with a honeycomb morphology represents a powerful strategy of composite design for metal fluorides in order to obtain exceptional electrochemical performance in metal fluoride Li batteries.

Overall, the results reported up to now display excellent potential for optimizing the architecture and composition of carbon-based metal fluoride cathodes to enhance their rate performance and cycling stability. Nevertheless, improving the electrochemical performance of carbon-based metal fluoride cathodes to the level of commercial applications still requires additional developments in novel fabrication techniques capable of precisely controlling the overall morphology and the nanoscale features of the carbon matrix and active materials. Therefore, more efforts are required to remove these issues for their commercialization.

Metal/metal oxide-based fluoride nanocomposites

Recently, the use of doping has been explored widely for intercalation-type electrode materials[111]. For conversion-type electrode materials, doping may also deliver obvious benefits to improve the ionic and electronic conductivities of electrode materials by enhancing the cathode performance through the intercalation of heterogeneous/homogenous metals, vacancies, or ions. Furthermore, many scientists have highlighted the possibility of decreasing the cluster size of creating "true" conversion electrode materials upon the lithiation process, attributed to the reduction in the interfacial energy and modification of the ion mobility of the clusters. As a result, this may improve the energy efficiency and cyclic stability of such electrodes because the affinity of the slow and steady separation of the cluster size could be diminished and the voltage hysteresis for the charge/discharge could be mitigated by reducing the paths for mass transport. In several recent reports, doping with Si has significantly enhanced the electronic conductivities of the

electrode materials, with remarkable discharge capacity utilization obtained as a result[112].

Molybdenum bisulfide was ball milled with FeF_3 to improve its electrochemical properties[113]. The orthorhombic structured FeF_3/MoS_2 with a uniform morphology showed excellent electrochemical performance as a cathode material in LIBs. The initial discharge capacity of the material was 170 mAh g^{-1} at a 0.1C rate with a voltage range from 2.0 to 4.5 V, and it maintained a specific capacity of 83.1% after 30 cycles. FeF_3 with an orthorhombic structure was prepared by Wu *et al.*[87] via a liquid phase method using HF, $FeCl_3$, and NaOH as precursors. The obtained product was further ball milled with conductive V_2O_5 powder to obtain a FeF_3/V_2O_5 nanocomposite. The electrochemical properties of the prepared material showed a significant improvement after the addition of V_2O_5. The FeF_3/V_2O_5 nanocomposite exhibited good rate and cycle performance. A discharge capacity of 209 mAh g^{-1} was obtained at a retention rate of 0.1C and a voltage range of 2.0-4.5 V and was maintained after 30 cycles.

A TiO_2-coated $FeF_3{\cdot}0.33H_2O$ cathode material with a spherical morphology was prepared via a solvothermal method by Zhang *et al.*[114]. The nanosized $FeF_3{\cdot}0.33H_2O$ was coated with uniform TiO_2 with an average particle size of ~1.0 μm and good dispersion ability. The initial reversible capacity at the retention rate of 0.1C was 654 (discharging) and 522 (charging) mAh g^{-1}, respectively, with a voltage range of 1.5-4.5 V. After 200 cycles, a good stability of 264 mAh g^{-1} was maintained by the nanomaterial cathode, which demonstrated that the TiO_2 layer on iron fluoride could be a promising cathode material for LIBs. A novel core-shell $FeF_3@Fe_2O_3$ nanocomposite (100-150 nm) and tunable iron oxide (Fe_2O_3) were prepared via a simple heat treatment using fine structured FeF_3 as a precursor[115]. The as-synthesized FeF_3 and core-shell $FeF_3@Fe_2O_3$ nanocomposites were characterized and their electrochemical performance was studied. A comparison between the pristine FeF_3 and the $FeF_3@Fe_2O_3$ nanocomposite revealed a significant improvement in the electrochemical performance upon the *in situ* coating of Fe_2O_3, even when the coating amount was 0.6-5.2 wt.%.

Metal doping has a positive effect on the charge/discharge capacity of metal fluoride cathode materials. The doped metal can increase the Li-ion diffusion coefficient and improve the electrochemical performance of the electrode materials. Recently, copper-doped FeF_3 nanomaterials have been synthesized via a liquid-phase method[116]. The electrochemical reversibility of $Fe_{1-x}Co_xF_3$ (x = 0, 0.03, 0.05 or 0.07) materials was further enhanced by the addition of acetylene black via mechanical a ball-milling process to obtain $Fe_{1-x}CoxF_3/C$ nanocomposites. It showed a significant improvement in electrochemical performance with the introduction of cationic Co. The discharge capacities at retention rates of 1, 2, and 5C were 150, 140, and 125 mA h g^{-1} and maintained the capacity after 100 cycles as high as 92.0%, 92.2%, and 91.7%, respectively. Metal fluoride cathode materials can suffer from particle fracture during lithiation/delithiation in LIBs. To improve the cathode nanoparticle stability and overcome this phenomenon, Co doping has been carried out for FeF_3 in LIBs by Zhang *et al.*[117]. In this study, calculations for Co doping onto the hexagonal tungsten bronze structure were carried out successfully to form $Co_xFe_{1-x}F_3$ systems (x = 0.08, 0.17 or 0.25). The study showed a sharp decrease in the band after Co doping, which may be attributed to the presence of Co 3d impurity energy levels between the conduction and valence bands. A thermally stable Co-doped iron fluoride ($Fe_{0.9}Co_{0.1}F_3{\cdot}0.5H_2O$) was synthesized by a non-aqueous precipitation method as a cathode material for LIBs[118]. The thermogravimetric analysis shows that the cathode nanomaterial was stable until 243 °C, with the crystal structure collapsing beyond this temperature due to water content elimination. The Co-doped cathode material showed a high discharge capacity (227 mAh g^{-1}) during cell cycling and retained a reversible capacity of 150 mAh g^{-1} after 200 cycles.

A significant boost in the electrochemical performance of FeF_2 cathode materials was found after the addition of NiF_2 nanomaterials for LIBs by Huang *et al.*[119]. The data obtained revealed the precise control of morphology and composition of the desired FeF_2-NiF_2 nanoparticles and undesirably enhanced capacity fading of the electrochemical cell. In another study, the substitution of Ni with Cu was carried out for binary NiF_2 nanomaterials and their electrochemical performance was studied for LIBs[120]. From *in situ* TEM, the structure of different ternary metal fluorides with Cu substitution was observed and the results revealed that when the Cu substitution was from 1-25 wt.%, the areal expansion reduced during the first lithiation. Furthermore, due to the reversible reaction, the fluorine loss during the delithiation was also reduced, which proved Cu to be a better choice for substitution to improve the electrochemical performance. Recently, ternary metal fluorides, like $AgCuF_3$ and $CuxFe_{1-x}F_2$, have been used as cathode materials in LIBs by Li *et al.*[121]. Thin-film Cu-Fe-F (CFF) cathode materials were successfully grown *in situ* via a pulsed laser deposition method. The as-prepared CFF cathode material showed a high specific capacity of 420 mAh g^{-1} and good cyclic stability even after 100 cycles, which may be attributed to reversible structural rearrangement after delithiation powered by high-resolution TEM, *in situ* XPS, and selected electron diffraction techniques.

Voltage hysteresis

Hysteresis is a common problem between the charge and discharge potentials in rechargeable batteries, which is related to thermodynamic and kinetic factors[9,10,18]. It may reduce capacity utilization and leads to low energy efficiency. In addition, the charge and discharge window with a larger voltage hysteresis may introduce more side reactions between the active substance and electrolyte and possibly unstable SEI. Unfortunately, MF cathodes show undesirably large voltage hysteresis, which is typically related to the poor electronic conductivity of the materials, rapid degradation of the battery, and changes in surface/interfacial energies during the conversion reactions. Energy losses for compensating the activation energies of breaking chemical bonds are also another key reason for voltage hysteresis. The discharge process (lithiation) of MF cathodes involves breaking Fe-F bonds and forming lower free-energy compounds containing lithium. The products from discharge process, such as LiF (bonding energy of Li-F is 577 kJ mol^{-1}), are thermodynamically stable due to the large electronegativity difference between Li and F. The charge process (reverse reaction) is required to decompose LiF by breaking the stronger corresponding chemical bonds. This introduces a large activation energy barrier, which contributes to a large voltage hysteresis (overpotential). This large voltage hysteresis even leads to the misapprehension that cells based on conversion MF cathodes are only primary batteries, such as Li-CuF_2 battery systems[50,55,60].

Recently, Li *et al.*[48] employed *in situ* analytical techniques to correlate the voltage profile with intermediate phases of FeF_3, which involved the evolution and spatial distribution of intermediate phases during the discharge-charge process. The results show that the phase evolution in the electrode is symmetric during cycling. However, the spatial evolution of the electrochemically active phase controlled by the reaction kinetics is different. They found that the kinetics of the FeF_3 electrode in nature is the reason for the voltage hysteresis. It originates from the Ohmic voltage drop, overpotential, and different spatial distributions of active phases, as shown in Figure 8. Therefore, the large hysteresis can be alleviated through the reasonable optimization of the material and electrode microstructure.

Elemental doping is a promising approach for conversion-type materials to overcome the problem of voltage hysteresis. The ionic and electronic conductivities of the electrode material are enhanced by the introduction of homogeneous/heterogeneous metallic (non-metallic) ions or vacancies. For example, FeF_2 doped with Cu and FeF_3 doped with Co showed lower voltage hysteresis. The partial substitution of F with O in FeF_3 greatly improves the reaction kinetics, reduces voltage hysteresis, and exhibits excellent cycle performance over 100 cycles (for this chemistry). Recently, Wang *et al.* proposed a novel strategy to make

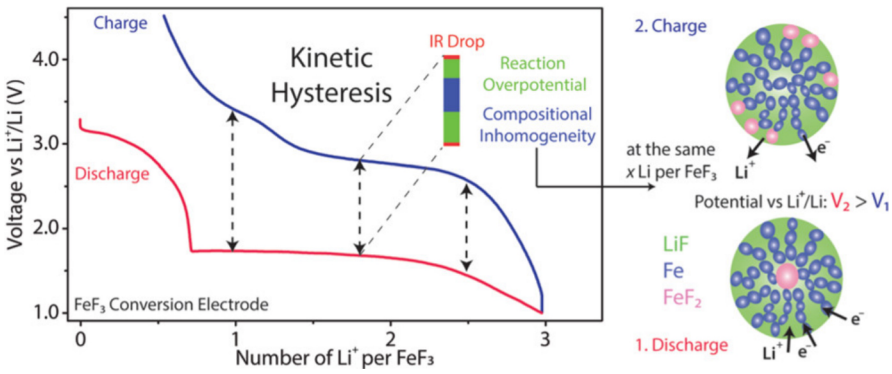

Figure 8. Schematic illustration of phase evolution in the electrode during discharge and charge. Reproduced from Ref.[48] with permission. Copyright 2016 American Chemical Society.

full use of the Cu^{2+}/Cu^{0} redox range for the first time in the application of copper-based fluorine rechargeable Li batteries[122]. The prepared FeF_2 (tetragonal rutile) and CuF_2 (monoclinal distorted rutile) solid solutions gave $Cu_{1-x}FexF_2$ a tetragonal rutile structure with high symmetry. It involves a two-stage lithiation process during the discharge process of the $Cu_{1-x}Fe_xF_2$ cathode. The first stage is at an upper plateau of ~2.9 V, which is related with a Cu-based conversion reaction, in a similar potential range as CuF_2. The second stage is at a higher potential of ~2.2 V, which is related with a Fe-based conversion reaction, as shown in Figure 9. $Cu_{0.5}Fe_{0.5}F_2$ displays a reversible capacity of 543 mAh g^{-1} at the first discharge-charge process. As-prepared cathode materials show enhanced dynamic performance, which lies in a reduction of the voltage hysteresis and the elimination of the voltage drop observed in FeF_2. After first-half conversion, the lattice disorder in FeF_2 increases due to the down-sizing of FeF_2, which is responsible for the disappearance of voltage drop and higher discharge voltage during the initial second-half conversion. There is a small voltage hysteresis of Cu^{2+}/Cu^{0} due to the low nucleation barrier for the formation/decomposition of the Cu-F bond.

Side reactions with electrolytes

The unfavorable side reactions between electrodes and electrolytes increase voltage hysteresis, reduce the Coulombic efficiency and stability of the cathode SEI and induce a safety hazard. There are multiple roles for the SEI, including limiting side reactions between the cathode (or anode) and the electrolyte. An ideal SEI layer has properties that include high cation conductance and electrical resistance, a thickness of a few nanometers, high mechanical toughness, and stability over a wide range of voltages. A stable SEI is an accepted prerequisite for safe battery performance, be it with a metal or an ion insertion anode. In theory, conversion-type cathodes should be advantageous in the thermodynamic stability of electrolytes because of their low electrochemical potentials (1.5-4.0 V *vs.* Li/Li^+). However, the oxidation stability of electrolytes can be changed by various salt anions, especially in concentrated electrolytes, and certain cathode chemicals. In addition, since the conversion cathode is usually discharged to a relatively low potential *vs.* Li/Li^+ (sometimes down to 1.2 V), the electrolyte may be reduced at the cathode surface. At moderate cathode potentials, the various substances formed by electrolyte reduction are more easily oxidized than the original electrolyte. Furthermore, some conversion cathode species may also catalyze the reduction reaction. For example, it has been found that the cyclic stability of MFs is worsened by the formation of a lithium carbonate species, which is susceptible to nanometal catalyzed reduction during the battery discharge to 1.2-2.0 V. The continuous large volume changes during cycling may prevent stabilization of the cathode SEI with poor elasticity in conversion-type cathodes. However, in contrast, the formation of a stable cathode SEI may also contribute to the stabilization of the conversion cathode, preventing adverse reactions between the cathode and electrolyte.

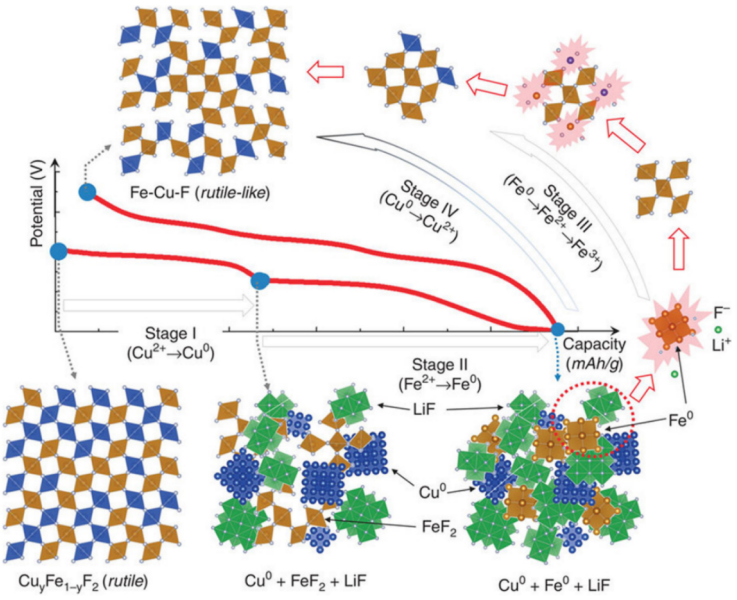

Figure 9. Illustration of potential reaction pathway of $Cu_{1-x}Fe_xF_2$ during discharge-charge. During discharge (stages I and II), Cu and Fe occur sequentially by the conversion reduction. During charge, the oxidation processes of Fe and Cu (stages III and IV) overlap to reform the disordered rutile-like Cu-Fe-F phase. Reproduced from Ref.[122] with permission. Copyright 2015 The Author(s).

In the case of liquid electrolytes, modifications have been made to the composition of lithium salts, organic solvents, salt concentrations, and organic and inorganic electrolyte additives in an attempt to alleviate the limitations of cathodes based on the conversion reaction. For intercalated cathodes and graphite anodes, classic organic carbonate esters are commonly used solvents, such as ethyl carbonate, propylene carbonate, ethyl carbonate, and ethyl carbonate. However, for the partial conversion of the cathode, the carbonate solvents may cause some adverse reactions. To address this problem, an electrolyte with a high concentration of LiTFSI salt has recently been developed to inhibit the dissolution of cathode materials by *in situ* forming a protective layer penetration on the surface of the electrode. In contrast, an ultrathin artificial SEI layer was prepared by atomic layer deposition, and it was reported that the conformation of the layer covered with fluorine particles reduced the side reaction between fluorine and the electrolyte. For example, 3D Al_2O_3-coated FeF_2 nanoparticles were prepared on Ni support by Kim *et al.*[83]. The results revealed that the electrochemical applications of the as-prepared electrode were significantly improved due to the ion transport pathway. The initial discharge capacity of the 3D FeF_2 electrode was 380 mAh g^{-1} at 200 mA g^{-1}. The reaction kinetics and specific capacity improved due to the 3D support, which makes an effective platform for electron transfer and shortening the Li-ion diffusion pathway. Therefore, more attention should be paid to the SEI to significantly improve the cyclic stability of metal fluorides.

SYNTHESIS OF METAL FLUORIDES

The reported results show excellent potential for improving the battery performance of metal fluoride cathodes by optimizing the composition and architecture of the cathode. However, in order to control the size features and morphology of the conversion-type cathode materials, novel synthesis technologies should be further developed to optimize the performance of cathode chemistries to the level of commercial applications. Metal fluoride electrodes have been prepared via different chemical and physical methods. The electrochemical performance of the metal fluoride cathode materials has shown significant improvements based on the specific synthesis method involved in forming nanoscale architectures. The low ionic and electronic conductivities of the metal fluorides can be improved either with homogenous mixing with a

highly conductive material or by reducing the particle size. Because nanoparticles can shorten the Li-ion diffusion time and provide a high surface area for contact with the electrolytes. Furthermore, nanostructured electrode materials have the ability to resist/hinder stress and strain from volume changes. The specific nanoscale morphology has proven to have an enormous impact on the specific capacity and cyclic stability of the electrode materials. In this section, the strategies employed to synthesize electrode materials are introduced, including hydrothermal, solvothermal, microwave synthesis, vapor-solid, ion synthesis and sol-gel methods.

Hydrothermal methods

Hydrothermal methods have often been used in synthetic chemistry due to the advantages of the crystalline powder at high temperatures. The controlled reaction conditions of the hydrothermal process result in the desired morphology[123-125]. In this process, the product prepared has good dispersion, high purity, uniform morphology and controlled particle size. It can be used to synthesize monocrystalline materials, as well as 2D and 3D materials, with particle sizes ranging from microns to nanometers.

The low electronic conductivity of FeF_2 cathode nanomaterials for LIBs was enhanced via the incorporation of ordered mesoporous carbon (CMK-3)[126]. The FeF_3 precursor was synthesized with the hydrothermal treatment of CMK-3 and iron oxide, followed by a topochemical process. The FeF_3 precursor was further annealed to obtain a hierarchical conductive FeF_2/CMK-3 nanoparticle network, as shown in Figure 10A. This type of hierarchical structure offers continuous electronic conduction within the network and porosity for the volume expansion of the prepared material. The prepared cathode material showed a stable cycle life of 1000 cycles with 0.3% capacity loss per cycle. After 100 cycles, high discharge capacities at current densities of 500, 2000, and 4000 mA g^{-1} were 500, 400, and 320 $mAhg^{-1}$, respectively, as shown in Figure 10B.

Solvothermal methods

Solvothermal methods are actually developed based on hydrothermal methods, except that the reaction medium is organic solvent rather than water. In a solvothermal process, one or more precursors in the reaction are dissolved under critical circumstances. This process has numerous advantages, including short reaction times, fast reaction kinetics, uniform particle distribution and high crystallinity. The electrode materials obtained by solvothermal methods have shown enhanced electrochemical performance, including good rate performance and long cycle life[127-129]. Recently, anhydrous CuF_2 nanomaterials from alkoxides $Cu(OR)_2$ (R = Me or tBu) were synthesized in hydrofluoric acid and tetrahydrofuran as reaction media[130]. A schematic diagram of the process is shown in Figure 11. Depending on the reaction conditions, different sizes of 10 and 100 nm nanoparticles were obtained. The product was found to be very hygroscopic and formed various hydrated products, including Cu(OH)F, $CuF_2{\cdot}2H_2O$, and $Cu_2(OH)F_3$. The as-prepared nanomaterials showed high electrochemical performance at a potential ~2.7 V for Li-ion charge/discharge. Different specific capacities were obtained with different particle sizes, e.g., 468 and 353 mAh g^{-1} for ~8 and ~12 nm crystalline diameters, respectively, for CuF_2. The high specific capacity of the nanomaterials faded after several cycles and the cell voltage decreased to 2.0 V, which was attributed to the irreversible nature of the reacting material involved in the electrochemical cell reaction.

In another study, $Fe_{(1-x)}Co_xF_3$/multi-walled carbon nanotube (MWCNT) nanocomposites were synthesized by a solvothermal method[131]. The iron fluoride nanomaterials doped with Co were wrapped with MWCNTs. The results of the prepared materials revealed the crystal structure adjustment, decreased the band gap, and enhanced the Li-ion diffusion capacity after Co doping. Moreover, the MWCNT wrapping increased the conductivity, which in turn enhanced the electrochemical performance of the $Fe_{0.96}Co_{0.04}F_3$ /MWCNT nanocomposites. The high specific capacity of the nanocomposites at 2.0-4.5 V recorded was 217.0 mAh g^{-1} at a rate of 0.2 C. The electrochemical performance was higher compared to the FeF_3

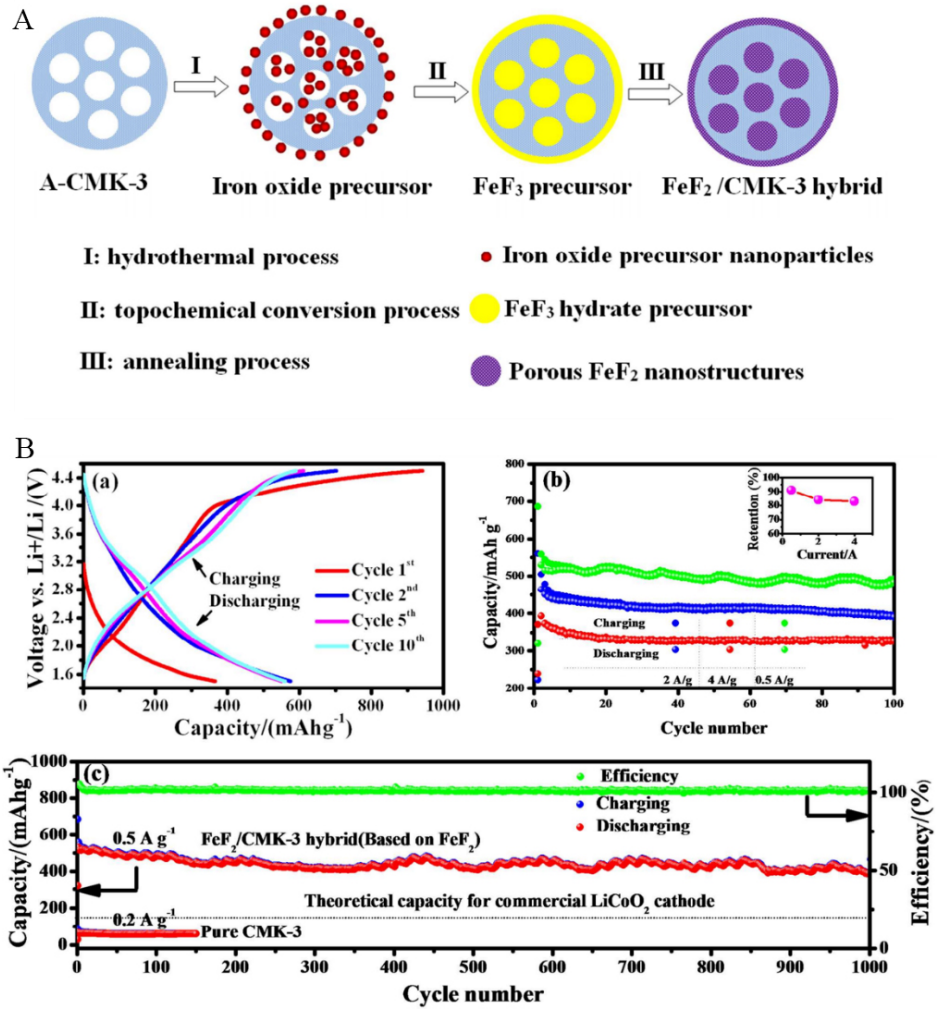

Figure 10. (A) Schematic illustration of the synthesis of porous FeF_2-CMK-3 composite. (B) Electrochemical performance of FeF_2 /CMK-3 cathodes: (a) charge-discharge profiles at 200 mAg^{-1}; (b) and (c) cycling performance. Reproduced from Ref.[126] with permission. Copyright 2015 Royal Society of Chemistry.

/MWCNT nanocomposite counterparts. After 50 cycles, the specific capacity of the two nanocomposites decreased to 187.9 and 160.7 mAh g^{-1}, respectively, which showed the cyclic stability of the prepared nanocomposites for Li storage in Li batteries.

Microwave-assisted methods

For the synthesis of metal fluoride nanomaterials, microwave-assisted approaches are promising routes compared to other synthetic methods. Since its first report in the field of synthetic chemistry and materials synthesis, this method has grown rapidly in this area of research[132]. By this method, the reaction entirely depends on the rapid heating, which produces reagents and solvents and makes this different from other methods, e.g., hydrothermal and solvothermal methods. Furthermore, the fast heated reaction results in a high reaction rate and efficiency and lower energy consumption[133]. In recent years, to obtain the tailorable morphologies, a combination of room-temperature ILs and a microwave heating process have been used[134]. A microwave-assisted approach was followed for the successful synthesis of self-assembled iron fluorides (HMIFs) with a hierarchical mesoporous structure[39]. The detailed possible steps and mechanism are shown in Figure 12. The dual nature fluorides, consisting of $FeF_3 \cdot H_2O$ and $Fe_{1.9}F_{4.75} \cdot 0.95H_2O$, were built

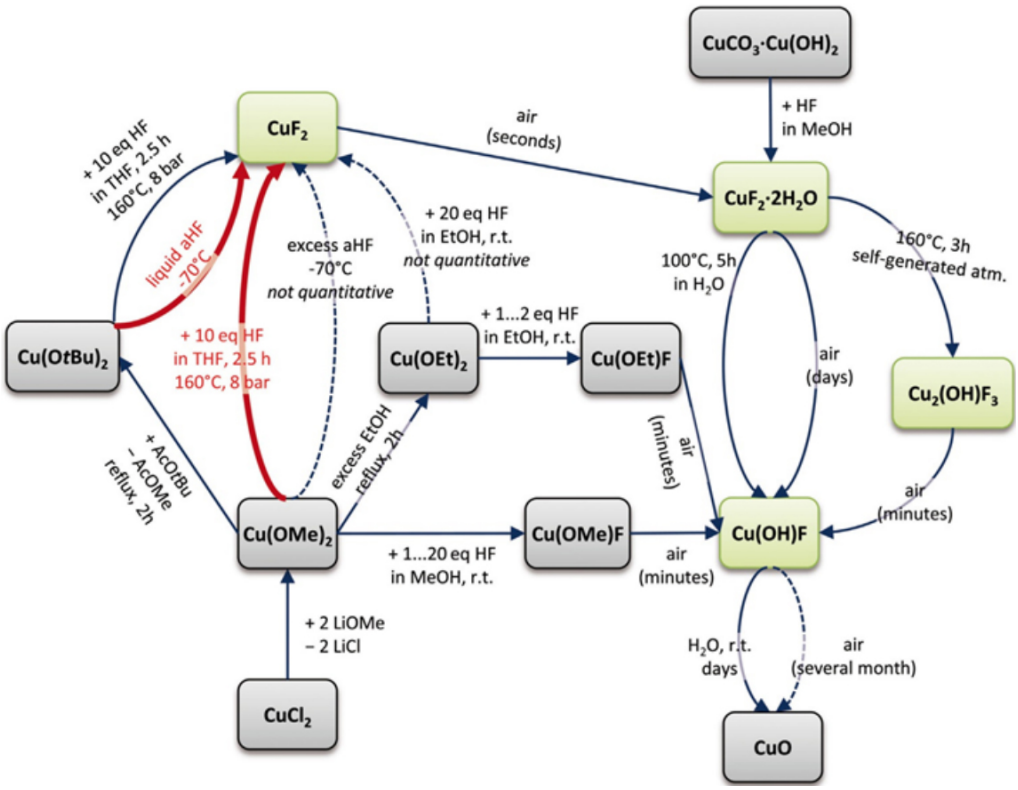

Figure 11. Overview of synthesis reactions. Thick red arrows represent most suitable reactions toward CuF_2. Dashed arrows represent product mixtures. Green boxes represent compounds used for electrochemical investigations. Reproduced from Ref.[130] with permission. Copyright 2018 Wiley VCH Verlag GmbH & Co. KGaA, Weinheim.

from a large number of nanorods with more than a dozen nanometer size and their electrochemical performance in LIBs investigated. The as-prepared HMIFs exhibited a homogeneous morphology with a hierarchical mesoporous structure and partial internal hollow core and possessed a specific area of 94 $m^2 g^{-1}$. By employing any conducting agent, the nanomaterials showed a high reversible capacity of 200 mA h g^{-1} and excellent cycle stability with a specific capacity of 148 mA h g^{-1} at 0.1C after 100 cycles. Moreover, the specific charge capacity exceeded 100 mA h g^{-1} at 5C, which showed the advancements of HMIF materials for high electrochemical performance applications in LIBs. This extraordinary performance was attributed to the formation of a unique structure that provided large storage sites for Li, as well as a large contact area for the electrode/electrolyte and hence a volume change during lithiation/delithiation and the facile mass transfer of electrons and Li ions during the electrochemical cell reaction.

Nanosized $NaFeF_3$ perovskite particles were synthesized from sodium ethoxide, ammonium fluoride and pre-synthesized FeF_2 rutile colloidal particles via a microwave-assisted method[135]. A schematic diagram, powder X-ray diffraction phases, which confirmed the expected crystal structure of rutile and orthorhombic-type crystal, and the 3D structure models are shown in Figure 13. The as-prepared perovskite $NaFeF_3$ nanomaterials showed excellent electrochemical performance with low polarization for Na and Li storage in energy storage devices. This enhanced performance of excellent capacity retention is attributed to the stable corner-sharing cubic Li and Na perovskite with stable cycle and low volume change and thermodynamic cost, as supported by a polymorphism theoretical study.

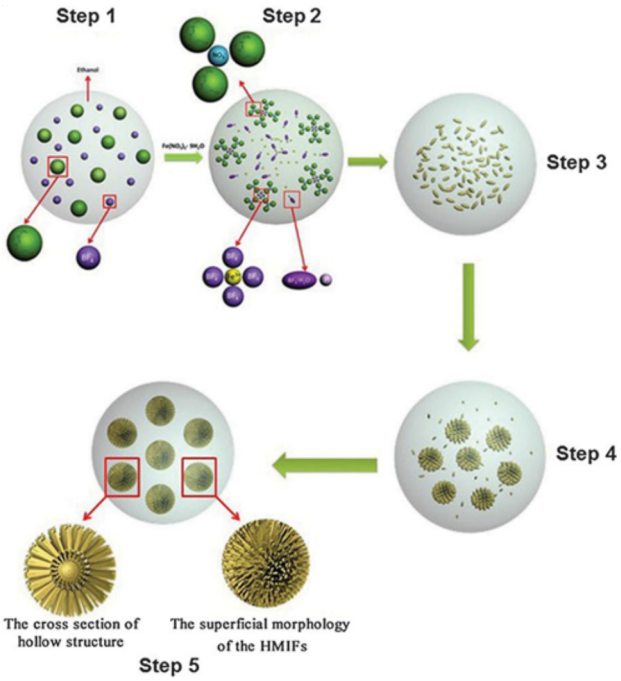

Figure 12. Schematic diagram of formation mechanism of partially hollow HMIFs. From steps 1 to 5: mixing the reactants; combining the solvated ions; initial stage emerging of nanoparticles; Ostwald ripening process; final state of the products. Reproduced from Ref.[39] with permission. Copyright 2014 Royal Society of Chemistry.

Sol-gel methods

Sol-gel methods are versatile routes in synthetic chemistry for designing complex nanostructures with controlled particle size, the arrangement of nanopores, and uniform particle distributions. The nanoporous behavior of the particle has the property of being functionalized during the gel formation even in a dry state by polymers or other active organic molecules. Upon careful heat treatment and utilization of the reaction precursor solution with temperature control, nanoparticles can be grown within the nanopores, which can be used in different applications with excellent performance[136]. There are some unique advantages of the sol-gel method, which make this process special compared to other conventional methods used for nanomaterial preparation. The first is the formation of a viscous solution from the dispersion of the raw materials during the process. A homogeneous mixture is achieved in a short period and even after the gel is formed, a molecular level homogeneous solution of the reactants is obtained. The second is that during the reaction, it is easy to add other materials, so molecular-level homogeneous doping is possible. The third is that the reaction can be carried out even at low temperatures and easily compared to the reaction involving solid components. This is because, in the sol-gel method, the reactants diffuse in the nanometer range, while for solid particles, the diffusion is at the micro level, and as a result, low temperature is required for the nanoscale formation.

FeF_3 nanocrystals as electrodes for LIBs with a particle size of 30 nm were prepared by a sol-gel method[137]. To enhance the electrochemical performance, the as-synthesized particles were fabricated with RGO, which shows a high specific retention of 150 mA h g^{-1} and stable cycle life for Li ions, even after 50 cycles. In another study, LiF- and FeF_2-based nanocomposites were prepared via a sol-gel method in ethanol for LIBs[138]. The SEM and TEM characterization of the LiF/FeF_2 composite proved that ~10 nm nanosized LiF and FeF_2 crystals were obtained, as shown in Figure 14A, with EDX and XRD analysis and a large surface area of 119 m^2 g^{-1}. The large surface and adsorption-desorption hysteresis revealed the presence of

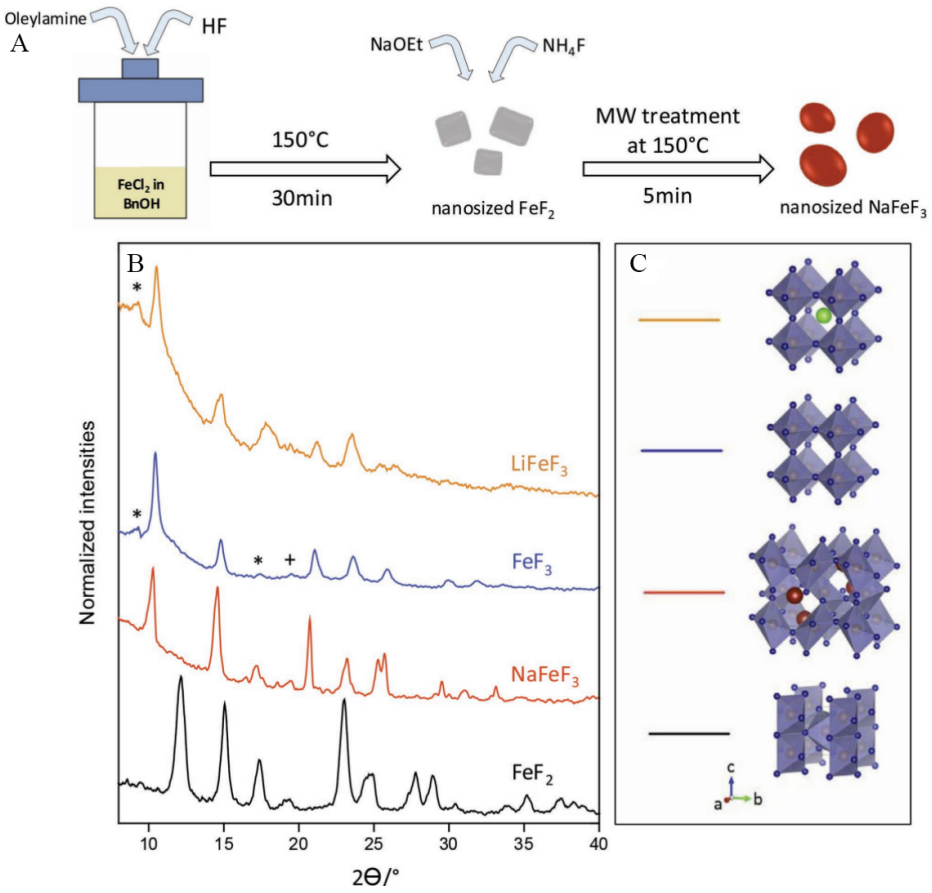

Figure 13. (A) Synthetic process of $NaFeF_3$ electrode material. (B) XRD patterns of as-prepared FeF_2 and $NaFeF_3$. (C) 3D structural models from XRD experiments. Reproduced from Ref.[135] with permission. Copyright 2019 Wiley VCH Verlag GmbH & Co. KGaA, Weinheim

mesopores, which might have a positive impact on the electrochemical performance. The initial discharge specific capacity of the reversible conversion reaction for the nanocomposites recorded was 225 mAh g^{-1} at a current rate of 10 mA g^{-1} with a stable life cycle, as shown in Figure 14B.

Ionothermal methods

Ionic liquids (ILs) have been discovered as alternatives to conventional solvents[139]. ILs are composed of cations and anions, in which one of them should be naturally organic and have a melting point below some arbitrary temperature[140]. This class of solvent is divided into two major groups based on their melting points, namely, room-temperature ILs, which melt at room temperature, and near room-temperature ILs, which have a melting point below 100 °C. Low vapor pressure is the distinguishing feature that makes them different from other solvents[141]. ILs were categorized as convenient alternatives to organic solvents much later, although they were recognized as solvents at the beginning of the 20th century. The main characteristics of ILs include good electric conductivity, fire resistance, high thermal stability, ability to dissolve many inorganic and organic compounds, nonvolatile, a wide range of temperatures, and recyclability[142,143]. These characteristics made ILs a good choice for energy storage devices. The *in situ* synthesis of FeF_3/GNS nanosheet hybrid nanomaterials was developed via an IL-assisted method[144]. The role of ILs was not only as green fluoride sources but also to provide uniform dispersion and tight surface modification of $FeF_3 \cdot 0.33H_2O$ on graphene nanosheets. The synthesis procedure of $FeF_3 \cdot 0.33H_2O$/GNS and

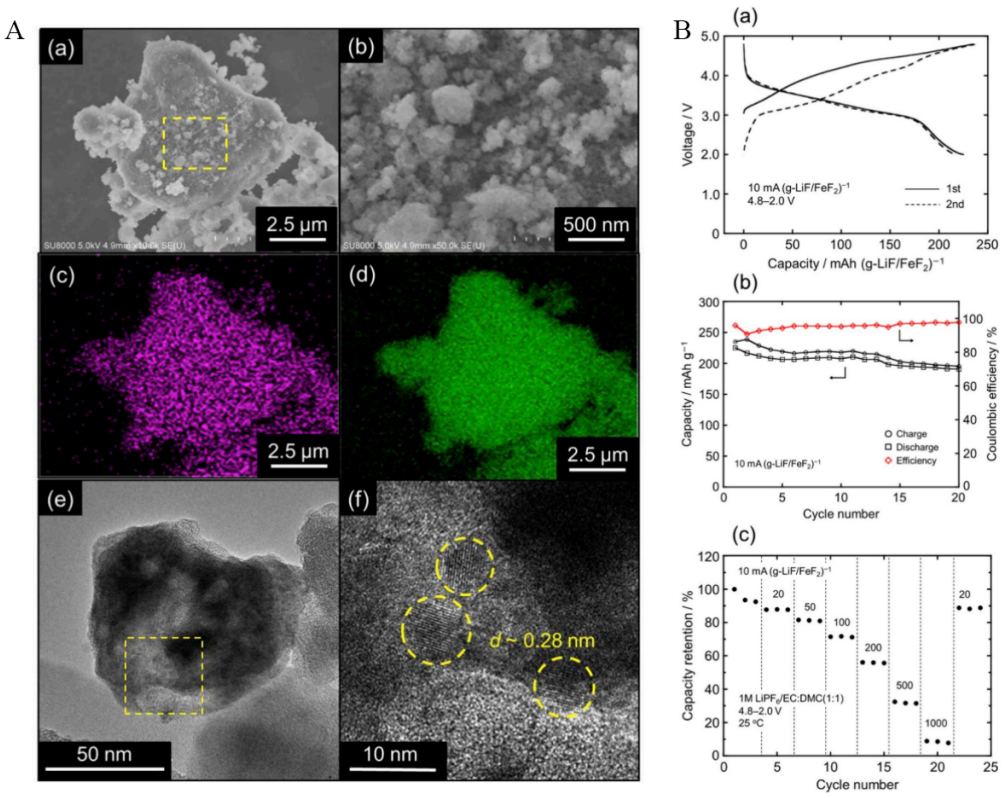

Figure 14. (A) (a) and (b) SEM images of LiF-FeF_2 composite. EDX mappings of (c) Fe and (d) F. (e) and (f) TEM images of LiF-FeF_2 electrode. (B) Charge-discharge performance: (a) charge-discharge profiles at current density of 10 mA g^{-1}; (b) cycling performance for first 20 cycles at 10 mA g^{-1}; (c) rate capability (from 10 to 1000 mA g^{-1}). Reproduced from Ref.[138] with permission. Copyright 2019 Elsevier B.V. All rights reserved.

the discharge profile at different currents are shown in Figure 15, where it can be seen that the as-synthesized $FeF_3 \cdot 0.33H_2O$/GNS cathode nanomaterials showed an extensive enhancement in both specific capacity and rate performance due to the electron transfer path of the iron nanoparticles and GNS in LIBs. The cyclic stability proves the strong adhesion of iron fluoride nanoparticles, which have a significant electrochemical performance of 115 mAh g^{-1} after 250 cycles, even at 10C, which is attributed to the strong structure of the hybrid and robust interaction between graphene and iron fluoride nanoparticles. In another study, mesoporous $FeF_3 \cdot 0.33H_2O$ cathode materials for LIBs were prepared at low temperatures via ILs as reaction media[23]. The enhanced electrochemical performance in terms of high reversible capacity and reactive voltage of the carbon free $FeF_3 \cdot 0.33H_2O$ cathode materials in LIBs was expected due to the morphology and optimization of hydration of the water-induced microstructure at room temperature.

Vapor-solid methods

A vapor-solid method was used to thermally convert Fe_3O_4/graphene into FeF_3/G cathode materials for LIBs[145]. This method has several advantages and has been used to prepare MF electrode materials for energy storage devices. This versatile method can be applied to prepare FeF_3 and metal oxide cathodes from Fe oxides/hydroxides and can be used to fabricate M_xF_y or M_xF_y/G composites for LIBs. Furthermore, this process can resist the increase in particle size due to the electronegativity of Fe, whose particles grow rapidly after nucleation compared to other solution-based processes. The conversion rate of FeF_3 from Fe_3O_4/G is also high and the product yield is good. The fabrication of porous carbon materials was successfully achieved on FeF_3 to prepare FeF_3/C nanocomposites in a tailored autoclave via a vapor-solid method[99]. The phase changes during the reaction between the HF solution and precursors in an Ar atmosphere were

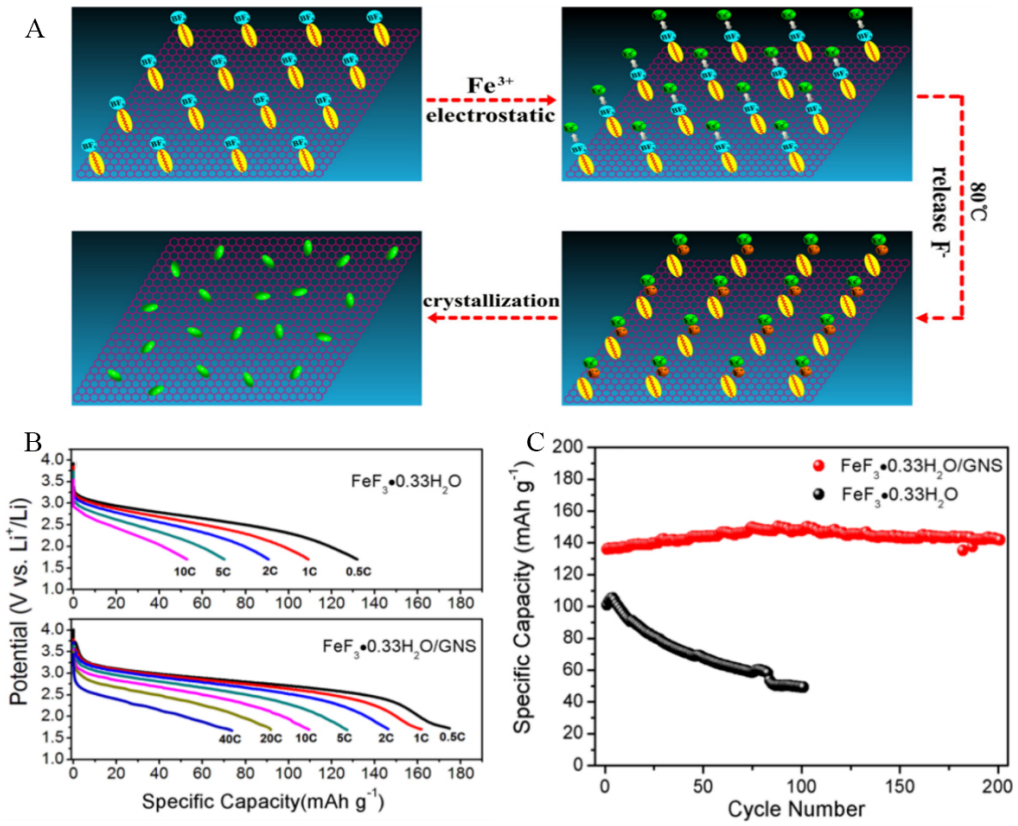

Figure 15. (A) Synthetic process of FeF_3·0.33H_2O/GNS composite. (B) Discharge profiles and (C) cycling performance of FeF_3·0.33H_2O/GNS composite and FeF_3·0.33H_2O without GNS. Reproduced from Ref.[144] with permission. Copyright 2013 American Chemical Society.

examined, and the results revealed that the autoclave had a vital role in driving the reaction to form FeF_3 nanomaterials. The charge capacity of the as-prepared FeF_3/C nanocomposites was 134.3, 103.2, and 71.0 mAh g^{-1} at different current densities of 100, 500, and 1000 mA g^{-1}, which are superior compared to the bare FeF_3 materials and displayed stable cyclic performance with a charge capacity of 200 mAh g^{-1}.

CURRENT CHALLENGES AND FUTURE OPPORTUNITIES

Metal fluorides have been used as electrode materials and offer significant advantages to rechargeable Li batteries with improved safety and low costs. Metal fluoride cathode materials give up to a 50% higher volumetric energy density and double the cell-level specific energy compared to other intercalation cathodes. However, the industrial application of metal fluoride conversion cathode materials is still limited due to several scientific challenges. These limitations include irreversible structural changes, volume change during cycling, active material dissolution, unfavorable interactions with electrolytes, large voltage hysteresis, and low electronic conductivity.

Some disadvantages of metal fluoride electrodes make them incongruous for practical energy storage devices. Firstly, in LIBs, the LiF produced during conversion reactions is highly insulated, which causes many problems during cycling, such as large voltage hysteresis and low electronic conductivity. Secondly, the volume changes during lithiation/delithiation can induce obvious decomposition of the SEI film. There have been several approaches to mitigate the challenges of metal fluoride electrode materials and make them promising choices for energy storage devices.

The conversion reactions of metal fluorides typically involve the breaking of bonds with transition metals, highly insulated products (e.g., LiF), and complicated reaction pathways. These features are responsible for cycling problems and voltage hysteresis. Although some reports have provided insight into such problems, more detailed insights are expected from advanced characterization and simulation tools. It is difficult to obtain deeper information from routine tools (such as TEM, SEM and XRD) due to the poorly crystallized conversion products. Therefore, advanced tools, such as PDF, NMR, EELS, TXM, and XAS, should be explored for studying conversion processes, which are sensitive to light elements and the finer microstructural details of the local structure.

The SEI is always an important but often neglected factor for the battery performance with metal fluoride cathodes. The SEI layer can become thicker during cycling, which causes the loss of active species and larger Fe interparticle distances, resulting in the capacity fade of the electrode. The growth of SEI layers is not desired for batteries as it can retard ionic and electronic transport. Artificial SEI layers (e.g., surface coatings) and optimizing the composition of the electrolyte, such as using a high concentration LiTFSI salt, may be efficient methods to solve these problems faced by the *in situ* formation of a protection layer at the electrode surface. In any case, SEI issues should be given more attention to obtaining good cycling stability.

One of the greatest challenges for metal fluorides is to improve their conversion energy efficiency by reducing the reaction overpotential. The energy density of FeF_3 is up to 1341.7 and 1899.13 Wh kg^{-1} during discharge and charge at 100 mA g^{-1}, respectively[146]. The conversion energy efficiency is only 70.7%, which is lower than the values for transition metal oxides (95.8% for NMC and 93.9% for $LiFePO_4$), as shown in Figure 16. To solve this problem, more focus should be devoted to the design of external wiring networks and the topological structure in future research. The surface defect chemistry (metastable or framework phases) of metal fluorides should also be considered to further optimize the spatial distribution of pristine phases, conversion products, and conductive network components in electrodes. One of the key tools is the defect chemistry of the involved phases including stoichiometric variations and doping. A promising method of improving the kinetics would use liquid-solid conversion mechanisms instead of the solid-solid conversion path. Therefore, it is worth studying conversion reactions involving Fe and $LiBF_4$ rather than LiF or considering boron-based additives as F^- receptors to dissociate LiF. Exploring electrolytes additives, separators and binders are also necessary for metal fluoride materials to suppress cathode dissolution effects and anode dendrite growth in the future.

In summary, the strategies for enhancing fluoride cathodes include: (1) the optimization of nanostructures for the formation of new desirable material, which will minimize the paths for Li ion diffusion and result in high electrochemical performance. An appropriate synthesis method could have a vital role in synthesizing desired nanoscale structures to obtain an advanced architecture of active metal fluoride materials; (2) achieving faster mass charge transport by building block and defect chemical variation in structures and (3) development or optimization of the electrolytes involved and the formation of advanced cell component solutions. It is obvious that to advance these electrode materials and make them ideal, numerous approaches have been employed to enhance the electrochemical performance, but significant improvements are still required for the practical applications of metal fluoride electrode materials.

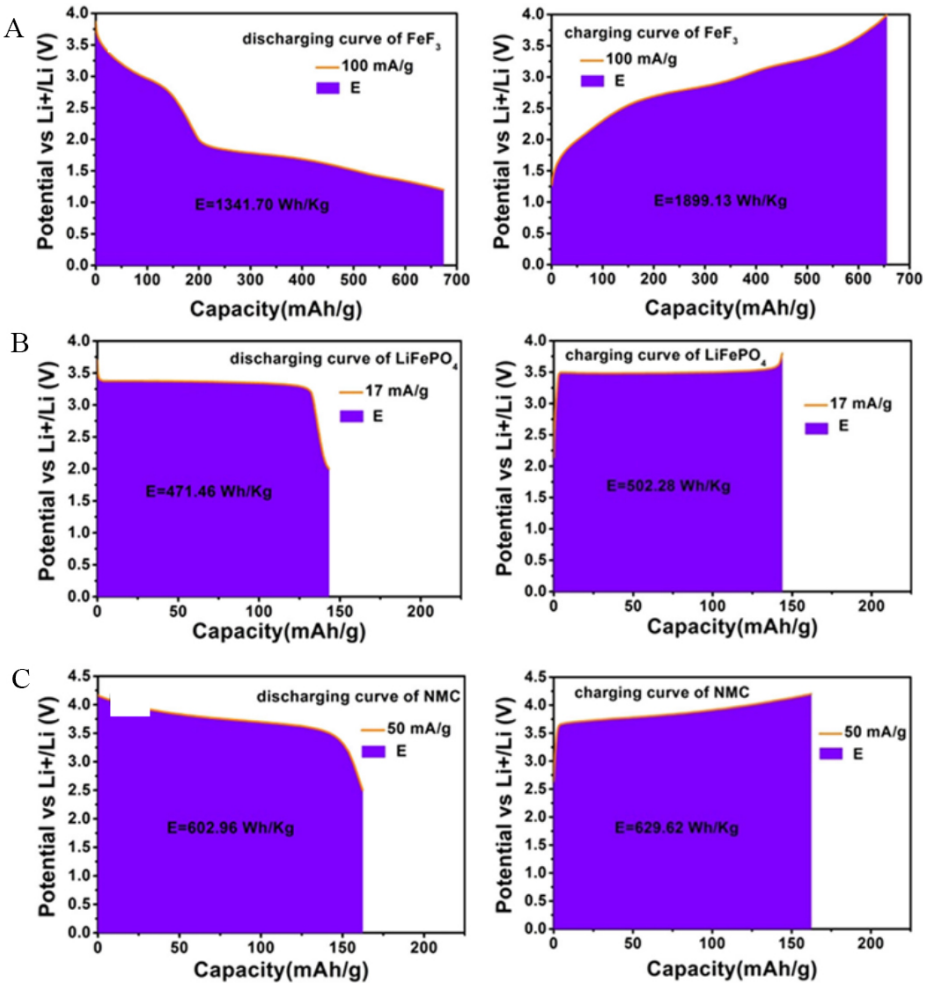

Figure 16. Energy efficiency and density of (A) FeF_3, (B) $LiFePO_4$ and (C) transition metal oxide (NMC) based on their discharge-charge curves. Reproduced from Ref.[146] with permission. Copyright 2018 The Author(s).

DECLARATIONS

Authors' contributions

Preparing the manuscript draft, writing-review, editing, funding acquisition: Ma D
Writing-review: Zhang R, Chen Y
Collecting literature: Xiao C, He F, Zhang S, Chen J
Funding acquisition, supervision: Hu X, Hu G

Availability of data and materials

Not applicable.

Financial support and sponsorship

This work was supported by the projects from National Natural Science Foundation of China (51802114, 21503008 and U2002213), Shandong Provincial Natural Science Foundation, China (ZR2019BF027). the Double Tops Joint Fund of the Yunnan Science and Technology Bureau and Yunnan University (2019FY003025), and Double First-Class University Plan (C176220100042). Key Discipline of Materials Science and Engineering, Chizhou University (czxyylxk03). Anhui Province materials and chemical industry first-class undergraduate talents demonstration leading base (2020rcsfjd28).

Conflicts of interest

All authors declared that there are no conflicts of interest.

Ethical approval and consent to participate

Not applicable.

Consent for publication

Not applicable.

Copyright

REFERENCES

1. Watanabe N. Two types of graphite fluorides, CF.n and C_2F.n, and discharge characteristics and mechanisms of electrodes of CF.n and C2F.n in lithium batteries. *Solid State Ionics* 1980;1:87-110. DOI
2. Feuillade G, Perche P. Ion-conductive macromolecular gels and membranes for solid lithium cells. *J Appl Electrochem* 1975;5:63-9. DOI
3. Wang L, Wu Z, Zou J, et al. Li-free cathode materials for high energy density lithium batteries. *Joule* 2019;3:2086-102. DOI
4. Dey AN. Experimental optimization of Li/$SOCl_2$ primary cells with respect to the electrolyte and the cathode compositions. *J Electrochem Soc* 1976;123:1262-1264. Available from: https://iopscience.iop.org/article/10.1149/1.2133057/meta [Last accessed on 26 Jul 2022.
5. Whittingham MS. Chemistry of intercalation compounds: metal guests in chalcogenide hosts. *Prog Solid State Chem* 1978;12:41-99. DOI
6. Xiao Q, Yang J, Wang X, et al. Carbon-based flexible self-supporting cathode for lithium-sulfur batteries: progress and perspective. *Carbon Energy* 2021;3:271-302. DOI
7. Hua X, Eggeman AS, Castillo-Martínez E, et al. Revisiting metal fluorides as lithium-ion battery cathodes. *Nat Mater* 2021;20:841-50. DOI PubMed
8. Xiao AW, Lee HJ, Capone I, et al. Understanding the conversion mechanism and performance of monodisperse FeF_2 nanocrystal cathodes. *Nat Mater* 2020;19:644-54. DOI PubMed
9. Karki K, Wu L, Ma Y, et al. Revisiting conversion reaction mechanisms in lithium batteries: lithiation-driven topotactic transformation in FeF_2. *J Am Chem Soc* 2018;140:17915-22. DOI PubMed
10. Wu F, Yushin G. Conversion cathodes for rechargeable lithium and lithium-ion batteries. *Energy Environ Sci* 2017;10:435-59. DOI
11. Castillo J, Qiao L, Santiago A, et al. Perspective of polymer-based solid-state Li-S batteries. *Energy Mater* 2022;2:200003. DOI
12. Tao J, Yan Z, Yang J, Li J, Lin Y, Huang Z. Boosting the cell performance of the SiO x @C anode material via rational design of a Si-valence gradient. *Carbon Energy* 2022;4:129-41. DOI
13. Yamakawa N, Jiang M, Key B, Grey CP. Identifying the local structures formed during lithiation of the conversion material, iron fluoride, in a Li ion battery: a solid-state NMR, X-ray diffraction, and pair distribution function analysis study. *J Am Chem Soc* 2009;131:10525-36. DOI PubMed
14. Li C, Mu X, van Aken PA, Maier J. A high-capacity cathode for lithium batteries consisting of porous microspheres of highly amorphized iron fluoride densified from its open parent phase. *Adv Energy Mater* 2013;3:113-9. DOI
15. Gu W, Magasinski A, Zdyrko B, Yushin G. Metal fluorides nanoconfined in carbon nanopores as reversible high capacity cathodes for Li and Li-ion rechargeable batteries: FeF_2 as an example. *Adv Energy Mater* 2015;5:n/a-n/a. DOI
16. Li L, Meng F, Jin S. High-capacity lithium-ion battery conversion cathodes based on iron fluoride nanowires and insights into the conversion mechanism. *Nano Lett* 2012;12:6030-7. DOI PubMed
17. Wang X, Gu W, Lee JT, et al. Carbon nanotube-CoF_2 multifunctional cathode for lithium ion batteries: effect of electrolyte on cycle stability. *Small* 2015;11:5164-73. DOI PubMed
18. Wang Y, Xu H, Zhong J, et al. Hierarchical Ni/Co-based oxynitride nanoarrays with superior lithiophilicity for high-performance lithium metal anode. *Energy Mater* 2021;1:100012. DOI
19. Li H, Richter G, Maier J. Reversible formation and decomposition of LiF clusters using transition metal fluorides as precursors and their application in rechargeable Li batteries. *Adv Mater* 2003;15:736-9. DOI
20. Ma D, Cao Z, Wang H, Huang X, Wang L, Zhang X. Three-dimensionally ordered macroporous FeF_3 and its in situ homogenous polymerization coating for high energy and power density lithium ion batteries. *Energy Environ Sci* 2012;5:8538. DOI
21. Makimura Y, Rougier A, Tarascon J. Pulsed laser deposited iron fluoride thin films for lithium-ion batteries. *Appl Surf Sci* 2006;252:4587-92. DOI
22. Zhang H, Zhou Y, Sun Q, Fu Z. Nanostructured nickel fluoride thin film as a new Li storage material. *Solid State Sci* 2008;10:1166-72. DOI

23. Li C, Gu L, Tsukimoto S, van Aken PA, Maier J. Low-temperature ionic-liquid-based synthesis of nanostructured iron-based fluoride cathodes for lithium batteries. *Adv Mater* 2010;22:3650-4. DOI PubMed
24. Gonzalo E, Kuhn A, García-alvarado F. On the room temperature synthesis of monoclinic Li_3FeF_6: a new cathode material for rechargeable lithium batteries. *J Power Sources* 2010;195:4990-6. DOI
25. Li C, Gu L, Tong J, Tsukimoto S, Maier J. A mesoporous iron-based fluoride cathode of tunnel structure for rechargeable lithium batteries. *Adv Funct Mater* 2011;21:1391-7. DOI
26. Cui Y, Xue M, Zhou Y, Peng S, Wang X, Fu Z. The investigation on electrochemical reaction mechanism of CuF_2 thin film with lithium. *Electrochim Acta* 2011;56:2328-35. DOI
27. Wang F, Robert R, Chernova NA, et al. Conversion reaction mechanisms in lithium ion batteries: study of the binary metal fluoride electrodes. *J Am Chem Soc* 2011;133:18828-36. DOI PubMed
28. Rangan S, Thorpe R, Bartynski RA, et al. Conversion reaction of FeF_2 thin films upon exposure to atomic lithium. *J Phys Chem C* 2012;116:10498-503. DOI
29. Liu P, Vajo JJ, Wang JS, Li W, Liu J. Thermodynamics and Kinetics of the Li/FeF_3 reaction by electrochemical analysis. *J Phys Chem C* 2012;116:6467-73. DOI
30. Zhao X, Hayner CM, Kung MC, Kung HH. Photothermal-assisted fabrication of iron fluoride-graphene composite paper cathodes for high-energy lithium-ion batteries. *Chem Commun* 2012;48:9909-11. DOI PubMed
31. Li C, Yin C, Gu L, et al. An FeF(3)·$0.5H_2O$ polytype: a microporous framework compound with intersecting tunnels for Li and Na batteries. *J Am Chem Soc* 2013;135:11425-8. DOI PubMed
32. Chu Q, Xing Z, Tian J, et al. Facile preparation of porous FeF_3 nanospheres as cathode materials for rechargeable lithium-ion batteries. *J Power Sources* 2013;236:188-91. DOI
33. Li C, Yin C, Mu X, Maier J. Top-down synthesis of open framework fluoride for lithium and sodium batteries. *Chem Mater* 2013;25:962-9. DOI
34. Parkinson MF, Ko JK, Halajko A, Sanghvi S, Amatucci GG. Effect of vertically structured porosity on electrochemical performance of FeF_2 films for lithium batteries. *Electrochim Acta* 2014;125:71-82. DOI
35. Duttine M, Dambournet D, Penin N, et al. Tailoring the composition of a mixed anion iron-based fluoride compound: evidence for anionic vacancy and electrochemical performance in lithium cells. *Chem Mater* 2014;26:4190-9. DOI
36. Tan J, Liu L, Hu H, et al. Iron fluoride with excellent cycle performance synthesized by solvothermal method as cathodes for lithium ion batteries. *J Power Sources* 2014;251:75-84. DOI
37. Li B, Cheng Z, Zhang N, Sun K. Self-supported, binder-free 3D hierarchical iron fluoride flower-like array as high power cathode material for lithium batteries. *Nano Energy* 2014;4:7-13. DOI
38. Lu Y, Wen ZY, Jin J, Wu XW, Rui K. Size-controlled synthesis of hierarchical nanoporous iron based fluorides and their high performances in rechargeable lithium ion batteries. *Chem Commun* 2014;50:6487-90. DOI PubMed
39. Lu Y, Wen Z, Jin J, Rui K, Wu X. Hierarchical mesoporous iron-based fluoride with partially hollow structure: facile preparation and high performance as cathode material for rechargeable lithium ion batteries. *Phys Chem Chem Phys* 2014;16:8556-62. DOI PubMed
40. Ma D, Wang H, Li Y, et al. In situ generated FeF_3 in homogeneous iron matrix toward high-performance cathode material for sodium-ion batteries. *Nano Energy* 2014;10:295-304. DOI
41. Hua X, Robert R, Du L, et al. Comprehensive study of the CuF_2 conversion reaction mechanism in a lithium ion battery. *J Phys Chem C* 2014;118:15169-84. DOI
42. Bao T, Zhong H, Zheng H, Zhan H, Zhou Y. In-situ synthesis of FeF_3/graphene composite for high-rate lithium secondary batteries. *Electrochim Acta* 2015;176:215-21. DOI
43. Zhao T, Li L, Chen R, et al. Design of surface protective layer of LiF/FeF_3 nanoparticles in Li-rich cathode for high-capacity Li-ion batteries. *Nano Energy* 2015;15:164-76. DOI
44. Hu X, Ma M, Mendes RG, et al. Li-storage performance of binder-free and flexible iron fluoride@graphene cathodes. *J Mater Chem A* 2015;3:23930-5. DOI
45. Li A, Wu S, Yang Y, Zhu Z. Structural and electronic properties of Li-ion battery cathode material MoF_3 from first-principles. *J Solid State Chem* 2015;227:25-9. DOI
46. Bai Y, Zhou X, Jia Z, et al. Understanding the combined effects of microcrystal growth and band gap reduction for Fe(1-)TiF_3 nanocomposites as cathode materials for lithium-ion batteries. *Nano Energy* 2015;17:140-51. DOI
47. Chen C, Xu X, Chen S, et al. The preparation and characterization of iron fluorides polymorphs FeF_3·$0.33H_2O$ and β-FeF_3·$3H_2O$ as cathode materials for lithium-ion batteries. *Mater Res Bull* 2015;64:187-93. DOI
48. Li L, Jacobs R, Gao P, et al. Origins of large voltage hysteresis in high-energy-density metal fluoride lithium-ion battery conversion electrodes. *J Am Chem Soc* 2016;138:2838-48. DOI PubMed
49. Jiang J, Li L, Xu M, Zhu J, Li CM. FeF_3@thin nickel ammine nitrate matrix: smart configurations and applications as superior cathodes for Li-ion batteries. *ACS Appl Mater Interfaces* 2016;8:16240-7. DOI PubMed
50. Rui K, Wen Z, Lu Y, Shen C, Jin J. Anchoring nanostructured manganese fluoride on few-layer graphene nanosheets as anode for enhanced lithium storage. *ACS Appl Mater Interfaces* 2016;8:1819-26. DOI PubMed
51. Hu J, Zhang Y, Cao D, Li C. Dehydrating bronze iron fluoride as a high capacity conversion cathode for lithium batteries. *J Mater Chem A* 2016;4:16166-74. DOI
52. Rao R, Pralong V, Varadaraju U. Facile synthesis and reversible lithium insertion studies on hydrated iron trifluoride FeF_3·$0.33H_2O$.

Solid State Sci 2016;55:77-82. DOI

53. Rui K, Wen Z, Jin J, Huang X. Controlled construction of 3D hierarchical manganese fluoride nanostructures via an oleylamine-assisted solvothermal route with high performance for rechargeable lithium ion batteries. *RSC Adv* 2016;6:27170-6. DOI
54. Sun H, Zhou H, Xu Z, Ding J, Yang J, Zhou X. Preparation of anhydrous iron fluoride with porous fusiform structure and its application for Li-ion batteries. *Microporous Mesoporous Mater* 2017;253:10-7. DOI
55. Li Y, Yao F, Cao Y, Yang H, Feng Y, Feng W. The mediated synthesis of FeF_3 nanocrystals through $(NH_4)_3FeF_6$ precursors as the cathode material for high power lithium ion batteries. *Electrochim Acta* 2017;253:545-53. DOI
56. Bai Y, Zhou X, Zhan C, et al. 3D Hierarchical nano-flake/micro-flower iron fluoride with hydration water induced tunnels for secondary lithium battery cathodes. *Nano Energy* 2017;32:10-8. DOI
57. Seo JK, Cho H, Takahara K, et al. Revisiting the conversion reaction voltage and the reversibility of the CuF_2 electrode in Li-ion batteries. *Nano Res* 2017;10:4232-44. DOI
58. Guntlin CP, Zünd T, Kravchyk KV, Wörle M, Bodnarchuk MI, Kovalenko MV. Nanocrystalline FeF_3 and MF_2 (M = Fe, Co, and Mn) from metal trifluoroacetates and their Li(Na)-ion storage properties. *J Mater Chem A* 2017;5:7383-93. DOI
59. Groult H, Neveu S, Leclerc S, et al. Nano-CoF_3 prepared by direct fluorination with F_2 gas: application as electrode material in Li-ion battery. *J Fluor Chem* 2017;196:117-27. DOI
60. Tong W, Amatucci GG. Silver copper fluoride: a novel perovskite cathode for lithium batteries. *J Power Sources* 2017;362:86-91. DOI
61. Zhang M. Fabrication of Li_2NiF_4-PEDOT nanocomposites as conversion cathodes for lithium-ion batteries. *J Alloys Compd* 2017;723:139-45. DOI
62. Yang Z, Zhao S, Pan Y, et al. Atomistic insights into FeF_3 nanosheet: an ultrahigh-rate and long-life cathode material for Li-ion batteries. *ACS Appl Mater Interfaces* 2018;10:3142-51. DOI PubMed
63. Zhai J, Lei Z, Rooney D, Wang H, Sun K. Self-templated fabrication of micro/nano structured iron fluoride for high-performance lithium-ion batteries. *J Power Sources* 2018;396:371-8. DOI
64. Zhao E, Borodin O, Gao X, et al. Lithium-iron (III) fluoride battery with double surface protection. *Adv Energy Mater* 2018;8:1800721. DOI
65. Li W, Groult H, Borkiewicz OJ, Dambournet D. Decomposition of CoF_3 during battery electrode processing. *J Fluor Chem* 2018;205:43-8. DOI
66. Jung S, Hwang I, Cho S, et al. New iron-based intercalation host for lithium-ion batteries. *Chem Mater* 2018;30:1956-64. DOI
67. Tang Z, Park JH, Kim SH, et al. Synthesis of Cu_7S_4 nanoparticles: role of halide ions, calculation, and electrochemical properties. *J Alloys Compd* 2018;764:333-40. DOI
68. Zhao Y, Wei K, Wu H, et al. LiF splitting catalyzed by dual metal nanodomains for an efficient fluoride conversion cathode. *ACS Nano* 2019;13:2490-500. DOI PubMed
69. Omenya F, Zagarella NJ, Rana J, et al. Intrinsic challenges to the electrochemical reversibility of the high energy density copper(II) fluoride cathode material. *ACS Appl Energy Mater* 2019;2:5243-53. DOI
70. Wang Q, Yang Z, Liu H, Wang X, Shi X. Atomically tailoring vacancy defects in $FeF_{2.2}(OH)_{0.8}$ toward ultra-high rate and long-life Li/Na-ion batteries. *J Mater Chem A* 2019;7:14180-91. DOI
71. Huang Q, Turcheniuk K, Ren X, et al. Insights into the effects of electrolyte composition on the performance and stability of FeF_2 conversion-type cathodes. *Adv Energy Mater* 2019;9:1803323. DOI
72. Chen G, Zhou X, Bai Y, et al. Enhanced lithium storage capability of $FeF_3{\cdot}0.33H_2O$ single crystal with active insertion site exposed. *Nano Energy* 2019;56:884-92. DOI
73. Zhu W, Chong S, Sun J, et al. The enhanced electrochemical performance of $Li_{1.2}Ni_{0.2}Mn_{0.6}O_2$ through coating MnF_2 nano protective layer. *Energy Technol* 2019;7:1900443. DOI
74. Zhou H, Sun H, Wang T, et al. Low temperature nanotailoring of hydrated compound by alcohols: $FeF_3{\cdot}3H_2O$ as an example. Preparation of NAnosized $FeF_3{\cdot}0.33H_2O$ cathode material for Li-ion batteries. *Inorg Chem* 2019;58:6765-71. DOI PubMed
75. Liu M, Liu L, Li M, et al. Preparation and Li/Na ion storage performance of raspberry-like hierarchical $FeF_3{\cdot}0.33H_2O$ micro-sized spheres with controllable morphology. *J Alloys Compd* 2020;829:154215. DOI
76. Kim SW, Seo DH, Gwon H, Kim J, Kang K. Fabrication of FeF_3 Nanoflowers on CNT branches and their application to high power lithium rechargeable batteries. *Adv Mater* 2010;22:5260-4. DOI PubMed
77. Badway F, Mansour AN, Pereira N, et al. Structure and electrochemistry of copper fluoride nanocomposites utilizing mixed conducting matrices. *Chem Mater* 2007;19:4129-41. DOI
78. Zhou H, Ruther RE, Adcock J, Zhou W, Dai S, Nanda J. Controlled formation of mixed nanoscale domains of high capacity Fe_2O_3-FeF_3 conversion compounds by direct fluorination. *ACS Nano* 2015;9:2530-9. DOI PubMed
79. Su H, Jiang Z, Liu Y, et al. Recent progress of sulfide electrolytes for all-solid-state lithium batteries. *Energy Mater* 2022;2:200005. DOI
80. Zhou J, Zhang D, Zhang X, Song H, Chen X. Carbon-nanotube-encapsulated FeF_2 nanorods for high-performance lithium-ion cathode materials. *ACS Appl Mater Interfaces* 2014;6:21223-9. DOI PubMed
81. Lee JT, Kim H, Oschatz M, et al. Micro- and mesoporous carbide-derived carbon-selenium cathodes for high-performance lithium selenium batteries. *Adv Energy Mater* 2015;5:1400981. DOI
82. Bashir T, Ismail SA, Song Y, et al. A review of the energy storage aspects of chemical elements for lithium-ion based batteries.

Energy Mater 2021;1:100019. DOI

83. Kim S, Liu J, Sun K, Wang J, Dillon SJ, Braun PV. Improved performance in FeF_2 conversion cathodes through use of a conductive 3D scaffold and Al_2O_3 ALD coating. *Adv Funct Mater* 2017;27:1702783. DOI
84. Levi MD, Aurbach D. Diffusion coefficients of lithium ions during intercalation into graphite derived from the simultaneous measurements and modeling of electrochemical impedance and potentiostatic intermittent titration characteristics of thin graphite electrodes. *J Phys Chem B* 1997;101:4641-7. DOI
85. Badway F, Cosandey F, Pereira N, Amatucci GG. Carbon metal fluoride nanocomposites. *J Electrochem Soc* 2003;150:A1318. DOI PubMed
86. Amatucci GG, Pereira N. Fluoride based electrode materials for advanced energy storage devices. *J Fluor Chem* 2007;128:243-62. DOI
87. Wu W, Wang Y, Wang X, et al. Structure and electrochemical performance of FeF_3/V_2O_5 composite cathode material for lithium-ion battery. *J Alloys Compd* 2009;486:93-6. DOI
88. Nishijima M, Gocheva ID, Okada S, Doi T, Yamaki J, Nishida T. Cathode properties of metal trifluorides in Li and Na secondary batteries. *J Power Sources* 2009;190:558-62. DOI
89. Concheso A, Santamaría R, Menéndez R, et al. Iron-carbon composites as electrode materials in lithium batteries. *Carbon* 2006;44:1762-72. DOI
90. Prakash R, Mishra AK, Roth A, et al. A ferrocene-based carbon-iron lithium fluoride nanocomposite as a stable electrode material in lithium batteries. *J Mater Chem* 2010;20:1871. DOI
91. Wang H, Maiyalagan T, Wang X. Review on recent progress in nitrogen-doped graphene: synthesis, characterization, and its potential applications. *ACS Catal* 2012;2:781-94. DOI
92. He C, Cheng J, Liu Y, Zhang X, Wang B. Thin-walled hollow fibers for flexible high energy density fiber-shaped supercapacitors. *Energy Mater* 2021;1:100010. DOI
93. Chang H, Wu Y, Han X, Yi T. Recent developments in advanced anode materials for lithium-ion batteries. *Energy Mater* 2021;1:100003. DOI
94. Atar N, Eren T, Yola ML, Gerengi H, Wang S. Fe@Ag nanoparticles decorated reduced graphene oxide as ultrahigh capacity anode material for lithium-ion battery. *Ionics* 2015;21:3185-92. DOI
95. Shao Y, Jin Z, Li J, Meng Y, Huang X. Evaluation of the electrochemical and expansion performances of the Sn-Si/graphite composite electrode for the industrial use. *Energy Mater* 2022;2:200004. DOI
96. Ma R, Lu Z, Wang C, et al. Large-scale fabrication of graphene-wrapped FeF_3 nanocrystals as cathode materials for lithium ion batteries. *Nanoscale* 2013;5:6338-43. DOI PubMed
97. Liu J, Wan Y, Liu W, et al. Mild and cost-effective synthesis of iron fluoride-graphene nanocomposites for high-rate Li-ion battery cathodes. *J Mater Chem A* 2013;1:1969-75. DOI
98. Qiu D, Fu L, Zhan C, Lu J, Wu D. Seeding iron trifluoride nanoparticles on reduced graphite oxide for lithium-ion batteries with enhanced loading and stability. *ACS Appl Mater Interfaces* 2018;10:29505-10. DOI PubMed
99. Ma R, Wang M, Tao P, et al. Fabrication of FeF_3 nanocrystals dispersed into a porous carbon matrix as a high performance cathode material for lithium ion batteries. *J Mater Chem A* 2013;1:15060. DOI
100. Kim YK, Lee JK, Kim J. FeF_3 Nanoparticles embedded in activated carbon foam (ACF) as a cathode material with enhanced electrochemical performance for lithium ion batteries: FeF_3/ACF nanocomposites as cathode. *Bull Korean Chem Soc* 2015;36:1878-84. DOI
101. Kim T, Jae WJ, Kim H, Park M, Han J, Kim J. A cathode material for lithium-ion batteries based on graphitized carbon-wrapped FeF_3 nanoparticles prepared by facile polymerization. *J Mater Chem A* 2016;4:14857-64. DOI
102. Huang T, Long M, Xiao JX, Liu H, Wang G. Recent research on emerging organic electrode materials for energy storage. *Energy Mater* 2021;1:100009. DOI
103. Mizushima K, Jones PC, Wiseman PJ, Goodenough JB. $LixCoO_2$ 0<x<-1.: a new cathode material for batteries of high energy density. *Mater Res Bull* 1980;15:783-789. DOI
104. Zhang L, Chen Y. Electrolyte solvation structure as a stabilization mechanism for electrodes. *Energy Mater* 2021;1:100004. DOI
105. Mishra A, Bäuerle P. Small molecule organic semiconductors on the move: promises for future solar energy technology. *Angew Chem Int Ed Engl* 2012;51:2020-67. DOI PubMed
106. Lu C, Dong C, Wu H, et al. Achieving high capacity hybrid-cathode $FeF_3@Li_2C_6O_6$/rGO based on morphology control synthesis and interface engineering. *Chem Commun* 2018;54:3235-8. DOI PubMed
107. Reddy MA, Breitung B, Kiran Chakravadhanula VS, et al. Facile synthesis of C-FeF_2 nanocomposites from CFx: influence of carbon precursor on reversible lithium storage. *RSC Adv* 2018;8:36802-11. DOI PubMed PMC
108. Fu W, Zhao E, Sun Z, Ren X, Magasinski A, Yushin G. Iron fluoride-carbon nanocomposite nanofibers as free-standing cathodes for high-energy lithium batteries. *Adv Funct Mater* 2018;28:1801711. DOI
109. Wu F, Chen S, Srot V, et al. A sulfur-limonene-based electrode for lithium-sulfur batteries: high-performance by self-protection. *Adv Mater* 2018;30:e1706643. DOI PubMed
110. Wu F, Srot V, Chen S, et al. 3D honeycomb architecture enables a high-rate and long-life iron (III) fluoride-lithium battery. *Adv Mater* 2019;31:e1905146. DOI PubMed
111. Yu R, Wang X, Fu Y, et al. Effect of magnesium doping on properties of lithium-rich layered oxide cathodes based on a one-step co-

precipitation strategy. *J Mater Chem A* 2016;4:4941-51. DOI

112. Luo C, Zhu Y, Wen Y, Wang J, Wang C. Carbonized polyacrylonitrile-stabilized SeS_x cathodes for long cycle life and high power density lithium ion batteries. *Adv Funct Mater* 2014;24:4082-9. DOI
113. Wu W, Wang X, Wang X, Yang S, Liu X, Chen Q. Effects of MoS_2 doping on the electrochemical performance of FeF_3 cathode materials for lithium-ion batteries. *Mater Lett* 2009;63:1788-90. DOI
114. Zhang R, Wang X, Wei S, Wang X, Liu M, Hu H. Iron fluoride microspheres by titanium dioxide surface modification as high capacity cathode of Li-ion batteries. *J Alloys Compd* 2017;719:331-40. DOI
115. Zhang W, Ma L, Yue H, Yang Y. Synthesis and characterization of in situ Fe_2O_3-coated FeF_3 cathode materials for rechargeable lithium batteries. *J Mater Chem* 2012;22:24769. DOI
116. Liu L, Zhou M, Yi L, et al. Excellent cycle performance of Co-doped FeF_3/C nanocomposite cathode material for lithium-ion batteries. *J Mater Chem* 2012;22:17539. DOI
117. Zhang Z, Yang Z, Li Y, Wang X. Revealing the doping mechanism and effect of cobalt on the HTB-type iron fluoride: a first-principle study. *J Phys Chem Solids* 2018;123:87-96. DOI
118. Ali G, Rahman G, Chung KY. Cobalt-doped pyrochlore-structured iron fluoride as a highly stable cathode material for lithium-ion batteries. *Electrochim Acta* 2017;238:49-55. DOI
119. Huang Q, Pollard TP, Ren X, et al. Fading mechanisms and voltage hysteresis in FeF_2 -NiF_2 solid solution cathodes for lithium and lithium-ion batteries. *Small* 2019;15:e1804670. DOI PubMed
120. Villa C, Kim S, Lu Y, Dravid VP, Wu J. Cu-substituted NiF_2 as a cathode material for Li-ion batteries. *ACS Appl Mater Interfaces* 2019;11:647-54. DOI PubMed
121. Li J, Xu L, Wei K, et al. In situ forming of ternary metal fluoride thin films with excellent Li storage performance by pulsed laser deposition. *Ionics* 2020;26:3367-75. DOI
122. Wang F, Kim SW, Seo DH, et al. Ternary metal fluorides as high-energy cathodes with low cycling hysteresis. *Nat Commun* 2015;6:6668. DOI PubMed PMC
123. Devaraju MK, Honma I. Hydrothermal and solvothermal process towards development of $LiMPO_4$ (M = Fe, Mn) nanomaterials for lithium-ion batteries. *Adv Energy Mater* 2012;2:284-97. DOI
124. Li C, Lin J. Rare earth fluoride nano-/microcrystals: synthesis, surface modification and application. *J Mater Chem* 2010;20:6831. DOI
125. Xiao Y, Xu R, Xu L, Ding J, Huang J. Recent advances on anion-derived sei for fast-charging and stable lithium batteries. *Energy Mater* 2021;1:100013. DOI
126. Song H, Cui H, Wang C. Extremely high-rate capacity and stable cycling of a highly ordered nanostructured carbon-FeF_2 battery cathode. *J Mater Chem A* 2015;3:22377-84. DOI
127. Zhang H, Yu X, Guo D, et al. Synthesis of bacteria promoted reduced graphene oxide-nickel sulfide networks for advanced supercapacitors. *ACS Appl Mater Interfaces* 2013;5:7335-40. DOI PubMed
128. Zhang Q, Zhang Y, Yin Y, Fan L, Zhang N. Packing $FeF_3 \cdot 0.33H_2O$ into porous graphene/carbon nanotube network as high volumetric performance cathode for lithium ion battery. *J Power Sources* 2020;447:227303. DOI
129. Tang Y, An J, Xing H, et al. Synthesis of iron-fluoride materials with controlled nanostructures and composition through a template-free solvothermal route for lithium ion batteries. *New J Chem* 2018;42:9091-7. DOI
130. Krahl T, Marroquin Winkelmann F, Martin A, Pinna N, Kemnitz E. Novel synthesis of anhydrous and hydroxylated CuF_2 nanoparticles and their potential for lithium ion batteries. *Chemistry* 2018;24:7177-87. DOI PubMed
131. Li J, Xu S, Huang S, Lu L, Lan L, Li S. In situ synthesis of $Fe_{(1-x)}Co_xF_3$/MWCNT nanocomposites with excellent electrochemical performance for lithium-ion batteries. *J Mater Sci* 2018;53:2697-708. DOI
132. Zhu YJ, Chen F. Microwave-assisted preparation of inorganic nanostructures in liquid phase. *Chem Rev* 2014;114:6462-555. DOI PubMed
133. Tsuji M, Hashimoto M, Nishizawa Y, Kubokawa M, Tsuji T. Microwave-assisted synthesis of metallic nanostructures in solution. *Chemistry* 2005;11:440-52. DOI PubMed
134. Ding K, Miao Z, Liu Z, et al. Facile synthesis of high quality TiO_2 nanocrystals in ionic liquid via a microwave-assisted process. *J Am Chem Soc* 2007;129:6362-3. DOI PubMed
135. Martin A, Doublet M, Kemnitz E, Pinna N. Reversible sodium and lithium insertion in iron fluoride perovskites. *Adv Funct Mater* 2018;28:1802057. DOI
136. Mackenzie JD, Bescher EP. Chemical routes in the synthesis of nanomaterials using the sol-gel process. *Acc Chem Res* 2007;40:810-8. DOI PubMed
137. Carlo L, Conte DE, Kemnitz E, Pinna N. Microwave-assisted fluorolytic sol-gel route to iron fluoride nanoparticles for Li-ion batteries. *Chem Commun* 2014;50:460-2. DOI PubMed
138. Tawa S, Sato Y, Orikasa Y, Matsumoto K, Hagiwara R. Lithium fluoride/iron difluoride composite prepared by a fluorolytic sol-gel method: its electrochemical behavior and charge-discharge mechanism as a cathode material for lithium secondary batteries. *J Power Sources* 2019;412:180-8. DOI
139. Pividori MI, Merkoçi A, Alegret S. Dot-blot amperometric genosensor for detecting a novel determinant of beta-lactamase resistance in Staphylococcus aureus. *Analyst* 2001;126:1551-7. DOI PubMed
140. Pópolo MG, Voth GA. On the structure and dynamics of ionic liquids. *J Phys Chem B* 2004;108:1744-52. DOI

141. Carriazo D, Serrano MC, Gutiérrez MC, Ferrer ML, del Monte F. Deep-eutectic solvents playing multiple roles in the synthesis of polymers and related materials. *Chem Soc Rev* 2012;41:4996-5014. DOI PubMed
142. Wasserscheid P. Ionic liquids-new "solutions" for transition metal catalysis. *Angew Chem Int Ed* 2000;39:3772-3789. DOI PubMed
143. Ghandi K. A review of ionic liquids, their limits and applications. *Green Sustain Chem* 2014;04:44-53. DOI
144. Li B, Rooney DW, Zhang N, Sun K. An in situ ionic-liquid-assisted synthetic approach to iron fluoride/graphene hybrid nanostructures as superior cathode materials for lithium ion batteries. *ACS Appl Mater Interfaces* 2013;5:5057-63. DOI PubMed
145. Choi NS, Chen Z, Freunberger SA, et al. Challenges facing lithium batteries and electrical double-layer capacitors. *Angew Chem Int Ed* 2012;51:9994-10024. DOI PubMed
146. Li C, Chen K, Zhou X, Maier J. Electrochemically driven conversion reaction in fluoride electrodes for energy storage devices. *npj Comput Mater* 2018:4. DOI